Electronic Supplementary Information

Axially Chiral Indolenine Derived Chromophore Dimers and their Chiroptical Absorption and Emission Properties

Emely Freytag[a], Marco Holzapfel[a], Asim Swain[a], Gerhard Bringmann[a], Matthias Stolte[a,b], Frank Würthner[a.b], Christoph Lambert[a,b]*

a) Institut für Organische Chemie, Universität Würzburg, Am Hubland, 97074 Würzburg, Germany.

b) Center for Nanosystems Chemistry, Universität Würzburg, Theodor-Boveri-Weg, 97074 Würzburg, Germany.

* Email: christoph.lambert@uni-wuerzburg.de

Table of contents

1 Materials and Methods

1.1 NMR Spectroscopy

- Avance III HD 400 FT-Spectrometer (1H: 400.13 MHz, 13C: 100.61 MHz) with a Bruker Ultrashield magnet

- Avance III HD 400 FT-Spectrometer (1H: 400.03 MHz, 13C: 100.59 MHz) with a Bruker Ascend magnet

- Avance III HD 600 FT-Spectrometer (1H: 600.13 MHz, 13C: 150.90 MHz) with an Oxford Instruments magnet

- Avance III HD 600 FT-Spectrometer (1H: 600.43 MHz, 13C: 150.98 MHz) with a Bruker Ascend magnet

^{1}H and ^{13}C spectra were recorded using one of the spectrometers listed above in deuterated solvents (acetone-d_6, CD_2Cl_2, $CDCl_3$, dimethylsulfoxide-d_6, THF-d_8). All solvents were used as received. Chemical shifts are given in ppm relative to the residual solvent signal (^{1}H; CH_2Cl_2: δ 5.32 $CHCl_3$: δ 7.26, acetone: δ 2.05, dimethylsulfoxide: δ 2.50, THF: δ 1.72, 3.58; ^{13}C: CH_2Cl_2: δ 53.84, $CHCl_3$: δ 77.16, acetone: δ 29.87, dimethylsulfoxide: δ 39.52, THF: δ 67.21, 25.31). The abbreviations used for assigning the spin multiplicities and C-atoms are: s = singlet, d = doublet, t = triplet, m = multiplet, dd = doublet of doublet, td = triplet of doublet; prim = primary, sec = secondary, tert = tertiary, quart = quarternary. Overlapping signals of chemically non-equivalent protons in ^{1}H NMR spectra are given as (m‘). The coupling constants are given in Hertz (Hz). Order of description for ^{1}H NMR spectra: chemical shift (spin multiplicity, coupling constant, number of protons, assignment).

1.2 Mass Spectrometry

Mass spectra were recorded with a Bruker Daltonics autoflex II LRF or a Bruker Daltonics UltrafleXtreme (MALDI) in positive mode (POS) using a DCTB (trans-2-[3-(4-*tert*-butylphenyl)-2-methyl-2-propenylidene]malononitrile) matrix. High resolution mass spectra were recorded with a Bruker Daltonic microTOF focus (ESI). All mass spectra peaks are reported as m/z. For

calculation of the respective mass values of the isotopic distributions the software Compass 1.1 from Bruker Daltonics GmbH (Bremen, Germany) was used. Calculated (calc.) and measured (found) peak values refer to the most intense peak of the isotopic distributions.

1.3 Gel Permeations Chromatography (GPC)

Shimadzu Recycling Gel Permeation Chromatography

- Photodiode array detector (SPD-M20A, 190-800 nm)

- Card type system controller (CBM-20Alite)

- Liquid Chromatograph (LC-20AD)

- Degassing unit (DGU-20A3R)

- Shimadzu valve unit (FCV-20AH2)

- Fraction collector (FRC-10A)

- Shimadzu LCsolution (v. 1.25

- Preparative PSS columns (styrene-divinylbenzene-copolymer / 10µ / 20 × 600 mm / 50 Å,100 Å, 500 Å)

Gel permeation chromatography (GPC) was done using two columns from PSS. HPLC-DCM from Sigma Aldrich was used as eluent with a flow rate of 4 ml min^{-1}.

1.4 High Performance Liquid Chromatography (HPLC)

The same Shimadzu device as for GPC was used. The analytical columns used were Phenomenex LUX 5 µm Cellulose-4 and Phenomenex LUX 5 µm i-Amylose-3. HPLC-hexane, HPLC-iPrOH, HPLC-DCM and HPLC-THF from Sigma Aldrich were used as eluents with a flow rate of 1 ml min^{-1}.

1.5 Solvent Purification System (SPS)

Inert anhydrous solvent dispensing system

- Model: PS-MD-6/7-EN

- Drying Columns: dual purifying columns design / polystyrene / medium density / 101 × 635 mm / 4 L internal volume

- 29/30 stainless steel glassware adaptors

- Particle filter (7 micron)

- 17 l solvent reservoirs for (DCM, DMF, Et2O, toluene, THF)

HPLC grade and stabilizer free solvents were used to fill the reservoirs.

1.6 UV-vis-NIR and CD spectroscopy

- JASCO V670 UV/vis/NIR-Spectrophotometer
- Jasco J-810 CD spectrometer

Solvents for spectroscopic studies were of spectroscopic grade und used as received from Acros Organics. Absorption spectra were measured in quartz cuvettes with path lengths of 10 mm at 293 K with concentrations of ca. 2.0×10^{-5} M and referenced against the pure solvent.

1.7 CPL spectroscopy

- JASCO CPL-300/J-1500 hybrid spectrometer

The CPL measurements were performed at 20 °C at different optical densities (OD(λ_{max}) = 0.1, 0.2, 0.7). The values for g_{lum} were obtained from the integrated analysis software and the obtained CPL spectra were smoothed for better quality.

1.8 Fluorescence spectroscopy

- Edinburgh Instruments FLS980 fluorescence lifetime spectrometer, 450 W Xenon lamp/PMT (R928P)

Steady-state emission spectra were recorded at 298 K in 10 mm quartz cells from Starna. The emission and excitation spectra were measured with strongly diluted samples (OD@λ_{max}< 0.05) in order to prevent self-absorption. The absolute fluorescence quantum yields were determined with more concentrated samples (OD@λ_{max} ~ 0.25, 0.5, 1.0) in an integrating sphere. The observed fluorescence quantum yields were afterwards corrected for self-absorption applying the method of Bardeen et al.[1] Fluorescence lifetimes were determined by time-correlated single-photon counting (TCSPC). The samples were excited by a pulsed laser diode under magic angle conditions and the fluorescence was detected with a high-speed PMT detector (H10720). A reconvolution fit of the data (4096 channels) was conducted by measuring the instrument response function with a scatterer solution consisting of colloidal silicon in deionised water (LUDOX). The FAST software (version 3.4.2) was used to fit the decay curves with exponential decay functions.

2 Absorption spectroscopy

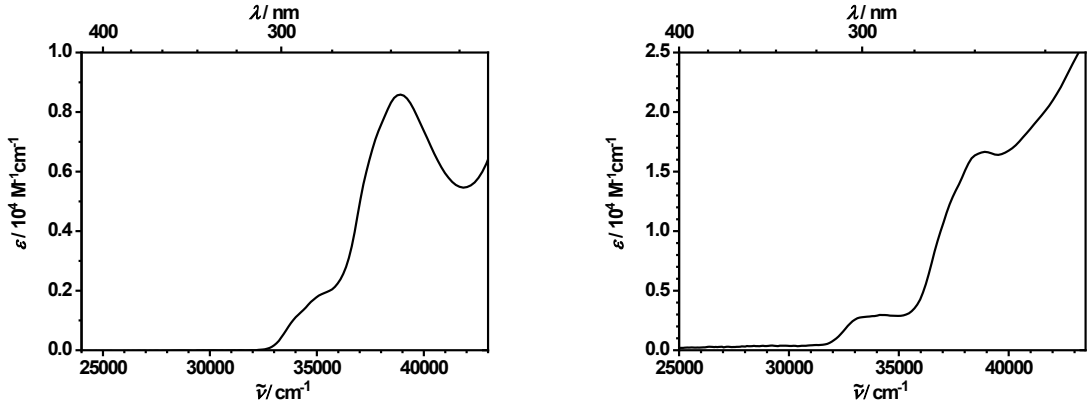

Fig. S1 UV-Vis spectra of **15** (left) and **8** (right) in DCM.

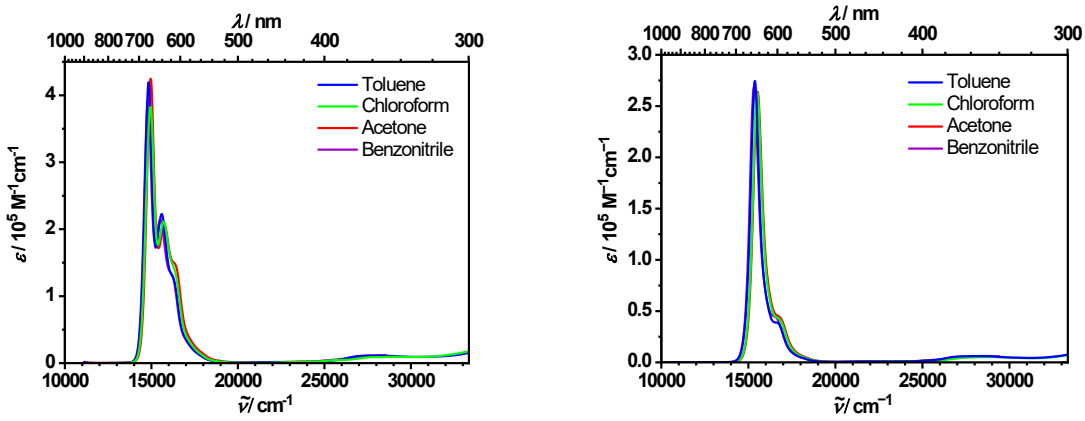

Fig. S2 UV-Vis spectra of **dSQA** (left) and **mSQA** (right) in various solvents.

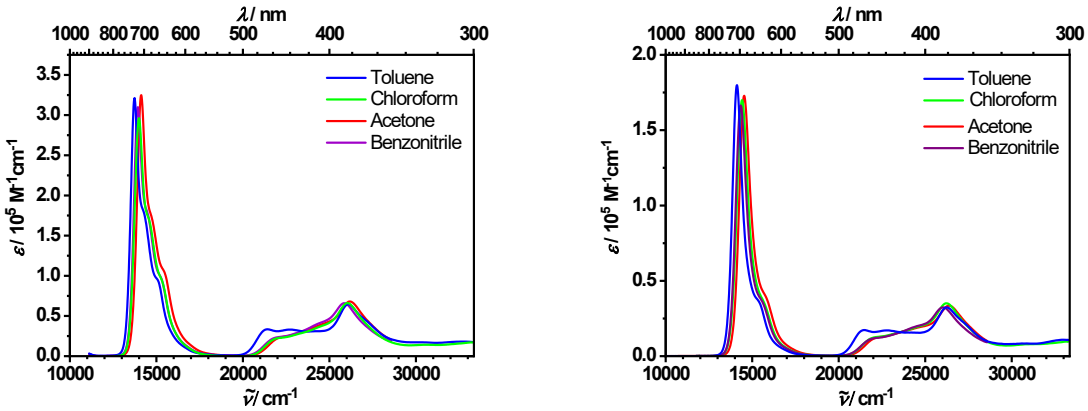

Fig. S3 UV-Vis spectra of **dSQB** (left) and **mSQB** (right) in various solvents.

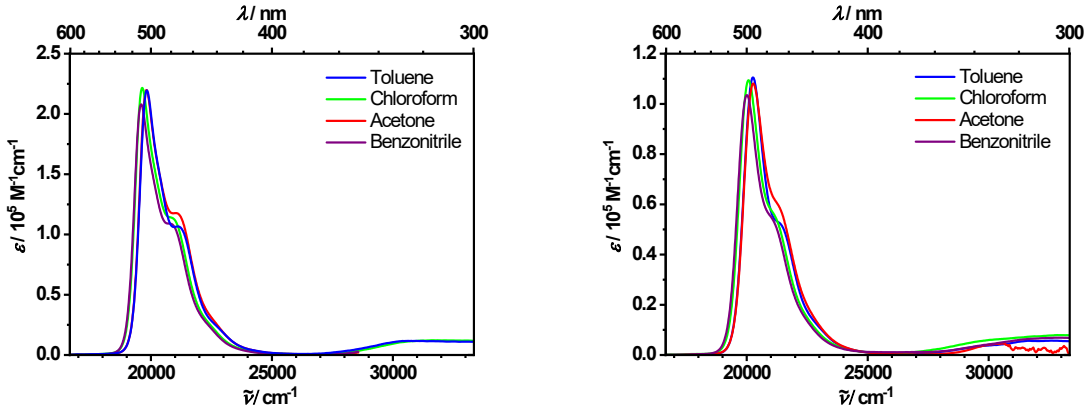

Fig. S4 UV-Vis spectra of **dMC** (left) and **mMC** (right) in various solvents.

Table S1 Spectroscopic data (absorption maxima and extinction coefficients of 1st and 2nd transition, average cubic fluorescence energy (see Eq. S4), quantum yields, fluorescence lifetimes) of **(*P*)-dSQA**, **(*P*)-dSQB**, **mSQA**, **mSQB**, **(*P*)-dMC**, **mMC** in toluene and chloroform.

	solvent	$\tilde{\nu}_{max1}$ / cm^{-1}	ε_{max1} / cm^{-1}	$\tilde{\nu}_{max2}$ / cm^{-1}	ε_{max2} / cm^{-1}	μ_{abs}^2 / D^2	$\tilde{\nu}_{av}$ / cm^{-1}	Φ_{fl}	τ_{fl} / ns
8	DCM	38900	1.67×10^4	-	-	-	-	-	-
15	DCM	38900	0.86×10^4	-	-	-	-	-	-
(*P*)-dSQA	toluene	14800	4.19×10^5	15600	2.22×10^5	222.5	14500	0.24	1.42 (0.59), 0.32 (0.41)
	chloroform	14900	3.83×10^5	15700	2.11×10^5	231.2	14500	0.14	0.63 (0.52), 0.23 (0.48)
(*P*)-dSQB	toluene	13700	3.21×10^5	14200	1.84×10^5	186.2	13300	0.52	3.06 (0.63), 1.47 (0.37)
	chloroform	14000	2.96×10^5	14500	1.74×10^5	187.6	13500	0.17	0.93 (0.36), 0.32 (0.64)
mSQA	toluene	15400	2.74×10^5	-	-	108.8	14900	0.36	1.23
	chloroform	15500	2.63×10^5	-	-	111.9	15000	0.43	1.35
mSQB	toluene	14100	1.80×10^5	-	-	88.5	13400	0.63	3.70
	chloroform	14400	1.70×10^5	-	-	93.2	13700	0.54	2.56
(*P*)-dMC	toluene	19800	2.20×10^5	20300	1.07×10^5	129.3	18600	0.07	0.16
	chloroform	19600	2.22×10^5	20100	1.14×10^5	137.6	18500	0.08	0.19
mMC	toluene	20200	1.11×10^5	-	-	62.8	18800	0.05	0.10
	chloroform	20100	1.09×10^5	-	-	66.8	18600	0.05	0.12

[a] Signal could not be measured completely and can therefore not be integrated

Table S2 Spectroscopic data (absorption transition dipole moments of the total exciton manifold, fluorescence lifetimes, average fluorescence lifetimes, radiative rate constants, non-radiative rate constants, transition dipole moments of S_1 and S_2 state and fluorescence transition dipole moments) of **(*P*)-dSQA**, **(*P*)-dSQB**, **(*R*)-mSQA**, **(*R*)-mSQB**, **(*P*)-dMC**, **(*R*)-mMC** in toluene.

	μ_{eg}^2 / D^2	τ_{fl} / ns[b]	$\bar{\tau}$fl / ns[b]	k_{fl} / 10^8 s^{-1} k_{nr} / 10^8 s^{-1}		$\mu_{S1}^{2\,a}$ / D^2	$\mu_{S2}^{2\,a}$ / D^2	μ_{fl}^2 / D^2
(*P*)-dSQA	222.5	1.42 (0.59), 0.32 (0.41)	0.97	2.48	10.3	137.5	85.0	85.8
(*P*)-dSQB	186.2	3.06 (0.63), 1.47 (0.37)	2.47	2.10	4.05	111.6	74.6	95.2
(*R*)-mSQA	108.8	1.23	1.23	2.93	8.13	-	-	94.4
(*R*)-mSQB	88.5	3.70	3.70	1.70	2.70	-	-	74.9
(*P*)-dMC	129.3	0.16	0.16	4.38	62.5	80.9	48.4	71.7
(*R*)-mMC	62.8	0.10	0.10	5.00	100.0	-	-	80.3

[a]The transition moments were estimated by assuming mirror image symmetry of the emission band shape and the S_1 absorption.

The following equation was used to calculate the squared transition dipole moments:

$$\mu_{eg}^2 = \frac{3hc\varepsilon_0 \ln(10) 9n}{2000\,\pi^2 N_A \left(n^2+2\right)^2} \int \frac{\varepsilon(\tilde{\nu})}{\tilde{\nu}} d\tilde{\nu} \qquad \text{(S1)}$$

Where $\hbar$ is the reduced Planck's constant, c is the speed of light in vacuum, ε_0 is the vacuum permittivity, N_A is Avogadro's constant, n is the refractive index of the solvent, $\tilde{\nu}$ is the wavenumber, $\varepsilon(\tilde{\nu})$ is the absorption coefficient dependent on the wavenumber.

The average lifetimes τ_{fl} were calculated by $\bar{\tau}_{fl}$

$$\bar{\tau}_{fl} = \frac{a_1\tau_1 + a_2\tau_2}{a_1 + a_2} \qquad \text{(S2)}$$

Here, a_n are the amplitudes and τ_n the corresponding lifetimes. The radiative rate constant k_{fl} was determined by equation S3.

$$k_{fl} = \frac{\phi_{fl}}{\bar{\tau}_{fl}} \qquad \text{(S3)}$$

In this equation, ϕ_{fl} is the fluorescence quantum yield. The squared transition dipole moments μ_{fl}^2 was obtained by the Strickler Berg equation, Eq S4.

$$k_f = \frac{16\times10^6\pi^3}{3h\varepsilon_0}\frac{n(n^2+2)^2}{9}\frac{g_g}{g_e}\left\langle\tilde{\nu}_{fl}^{-3}\right\rangle_{av}^{-1}\mu_{fl}^2 \quad \text{with} \quad \left\langle\tilde{\nu}_{fl}^{-3}\right\rangle_{av}^{-1} = \int I_f d\tilde{\nu} \Big/ \int \tilde{\nu}^{-3} I_f d\tilde{\nu} \qquad \text{(S4)}$$

3 CD spectroscopy

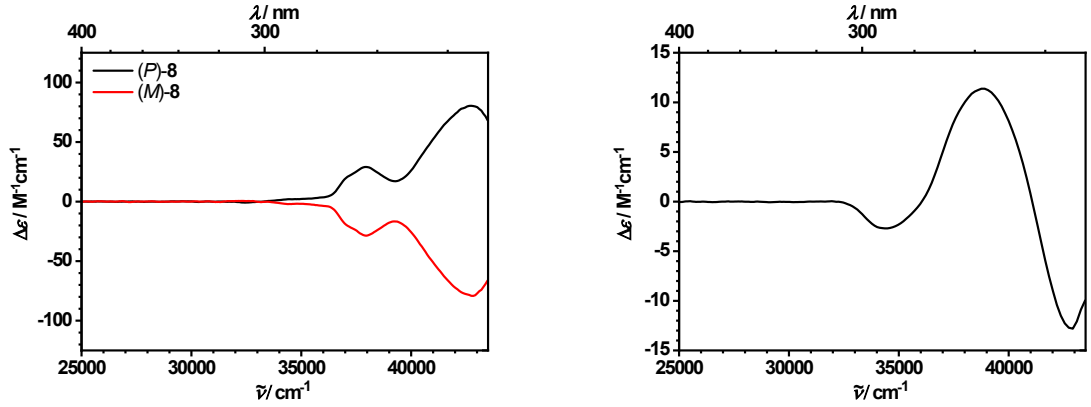

Fig. S5 ECD specta of **(*P*)-** and **(*M*)-8** (left) and **(*R*)-15** (right) in DCM.

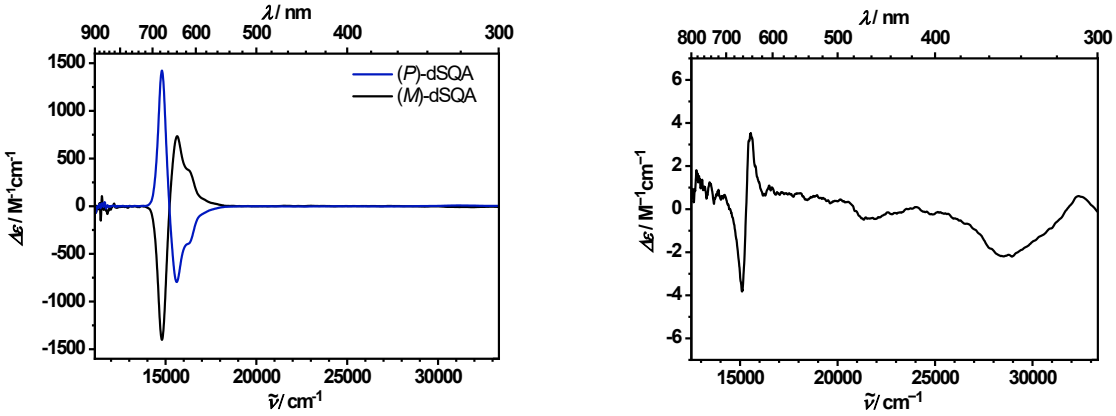

Fig. S6 ECD spectra of **(*P*)-** and **(*M*)-dSQA** (left) and **(*R*)-mSQA** (right) in toluene.

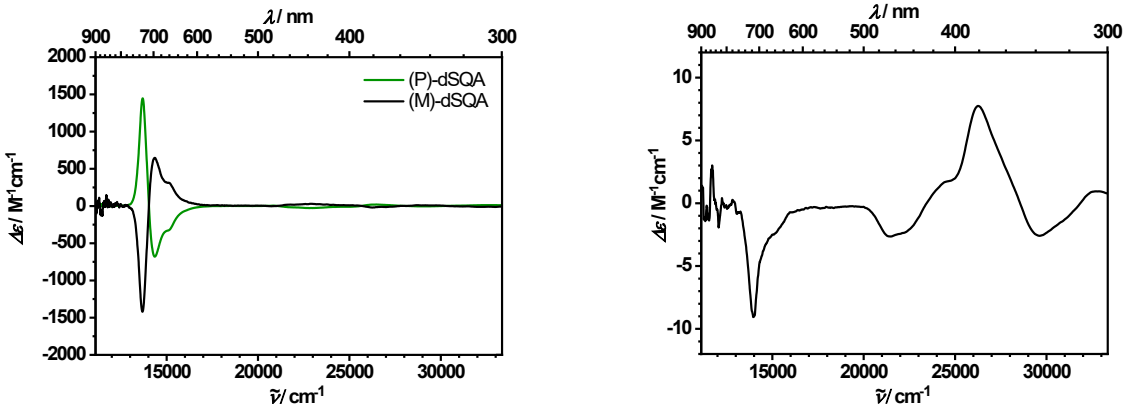

Fig. S7 ECD spectra of **(*P*)-** and **(*M*)-dSQB** (left) and **(*R*)- mSQB** (right) in toluene.

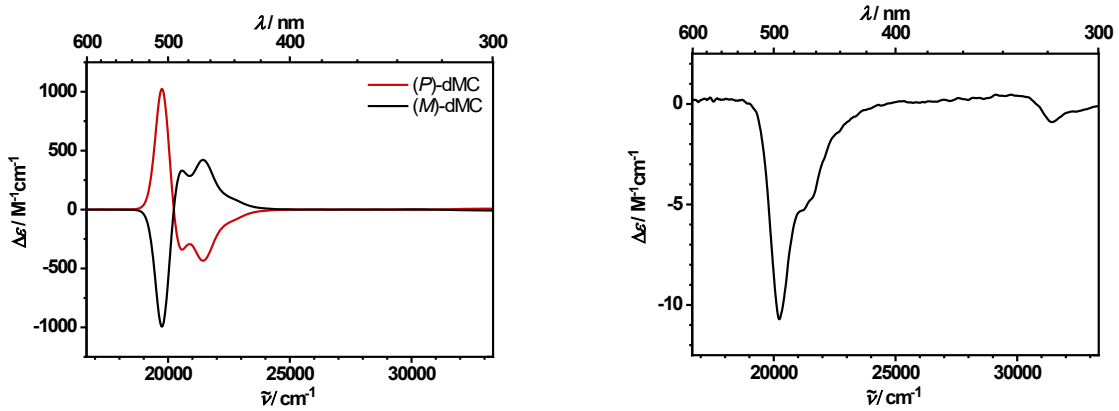

Fig. S8 ECD spectra of **(*P*)-** and **(*M*)-dMC** (left) and **(*R*)-mMC** (right) in toluene.

Table S3 Chiroptical data (ECD maxima, extinction coefficients, rotational strength and anisotropy factor) of **(*P*)-8** and **(*R*)-16** in DCM and **(*R*)-mSQA**, **(*R*)-mSQB** and **(*R*)-mMC** in toluene.

	$\tilde{\nu}_{max}$ / cm^{-1}	$\Delta\varepsilon$ / M^{-1}cm^{-1}	R_{exp} / 10^{-40} cgs	$\lvert g_{abs}(\tilde{\nu}_{max})\rvert$ / cgs[d]
(*P*)-8	37900	29.3	[b]	4.2 × 10^{-3}
	42800	80.8	[a]	3.4 × 10^{-3}
	34400	–2.7	–3.86	1.3 × 10^{-3}
(*R*)-15	38800	11.4	21.2	2.1 × 10^{-3}
	42900	–12.8	[a]	2.0 × 10^{-3}
(*R*)-mSQA	15100	–3.8	[b]	2.9 × 10^{-5}
	15600	3.5	[b]	1.9 × 10^{-5}
(*R*)-mSQB	14000	–9.0	–17.2	6.3 × 10^{-5}
	26000	7.7	15.4	2.4 × 10^{-4}
(*R*)-mMC	20200	–10.7	–19.5	9.7 × 10^{-5}

[a] Signal could not be measured completely and can therefore not be integrated; [b] Not determinable due to overlap of signals with opposite signs.

Following equation was used to calculate the experimental rotatory strengths:

$$R = \frac{3(2303)\hbar c}{16\pi^2 N_A}\int\frac{\Delta\varepsilon(\tilde{\nu})}{\tilde{\nu}}\mathrm{d}\tilde{\nu} \qquad \text{(S5)}$$

where $\Delta\varepsilon(\tilde{\nu})$ is the difference of absorption coefficients of right and left circularly polarised light dependent on the wavenumber.

4 TD-DFT calculations

All DFT and TD-DFT calculations were performed using the software package Gaussian09.[2] The structures were optimised at the B3LYP/6-31G* level. The TD calculations were then performed using these geometries at the BHandHLYP/6-31G* level.

4.1 Oscillator strengths

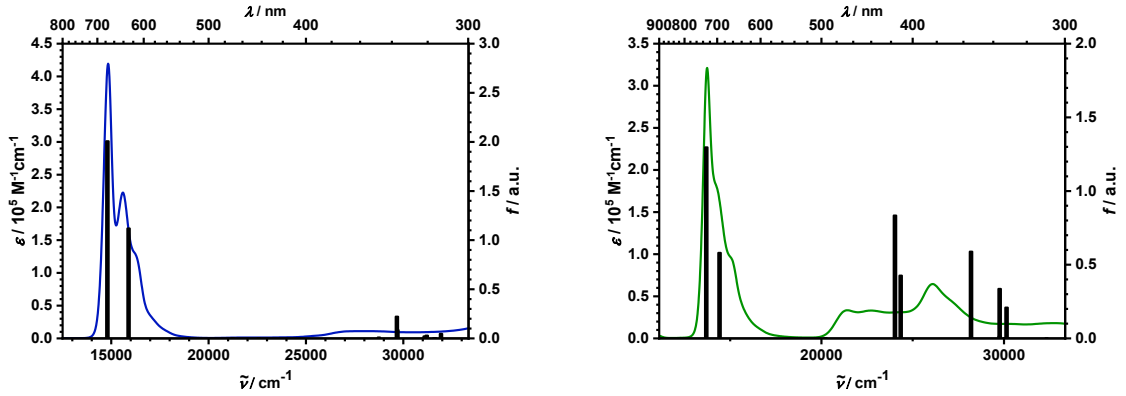

Fig. S9 TD-DFT calculated oscillator strengths of dimers at the BHandHLYP/6-31G* level. Left: **(*P*)-dSQA** (shifted by 4558 cm^{-1}), right: **(*P*)-dSQB** (shifted by 3378 cm^{-1}).

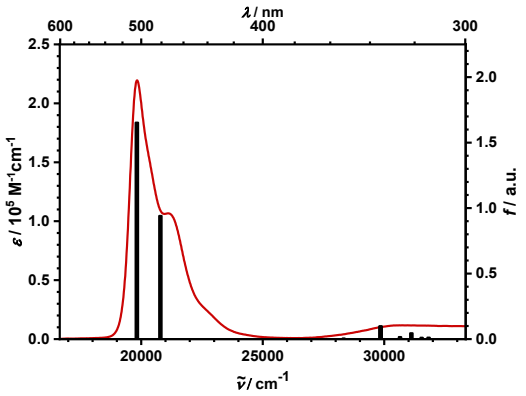

Fig. S10 TD-DFT calculated oscillator strength of **(*P*)-dMC** at the BHandHLYP/6-31G* level (shifted by 6916 cm^{-1}).

4.2 Rotational strengths

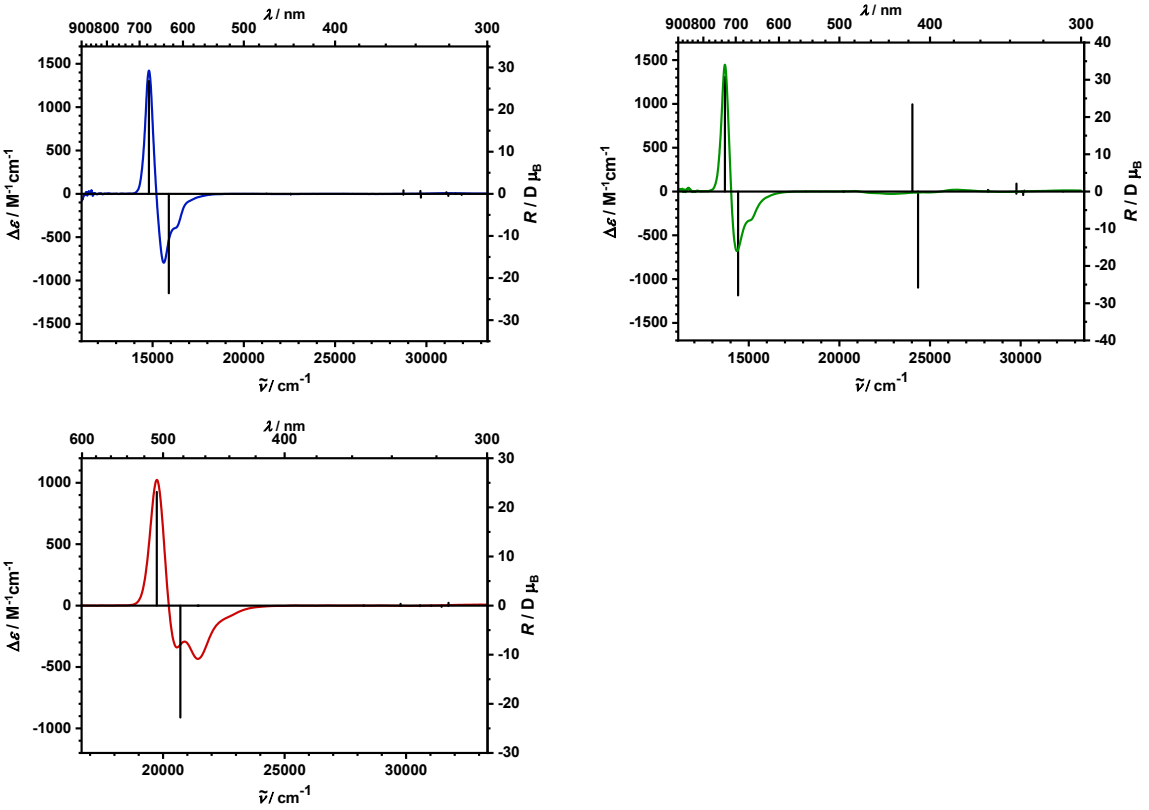

Fig. S11 TD-DFT calculated rotatory strengths (together with experimental spectra) of dimeric dyes at the BHandHLYP/6-31G* level with Gaussian distribution. Top left: **(*P*)-dSQA** (shifted by 4558 cm^{-1}), top right: **(*P*)-dSQB** (shifted by 3378 cm^{-1}), bottom left: **(*P*)-dMC** (shifted by 6916 cm^{-1}).

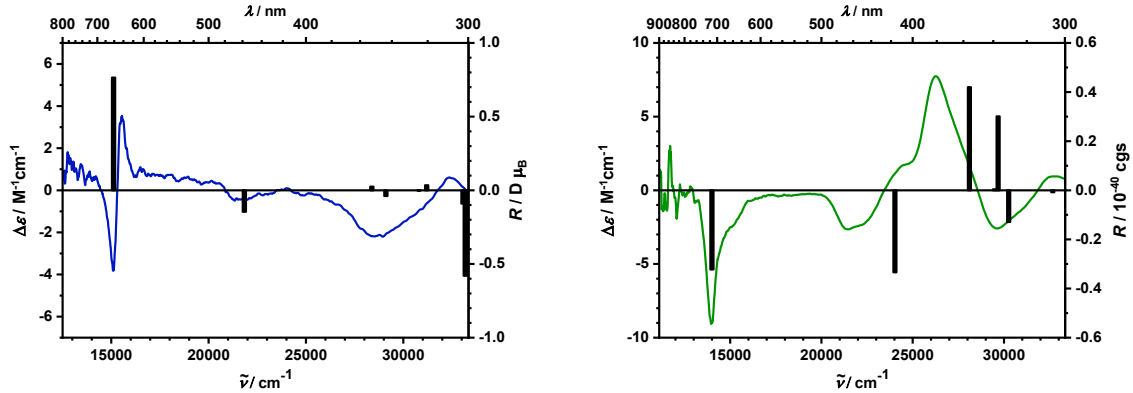

Fig. S12 TD-DFT calculated rotational strengths of monomers at the BHandHLYP/6-31G* level. Left: **(*R*)-mSQA** (shifted by 4558 cm^{-1}), right: **(*R*)-mSQB** (shifted by 3515 cm^{-1}).

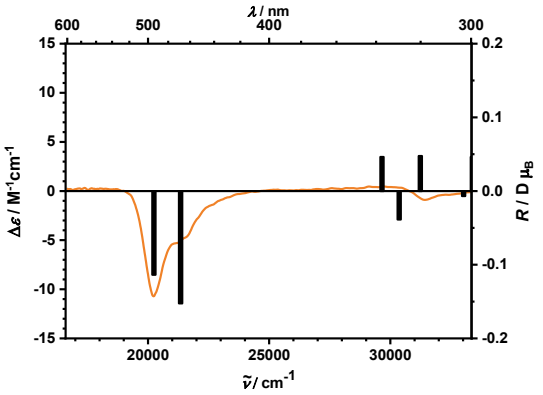

Fig. S13 TD-DFT calculated rotational strengths of **(*R*)-mMC** at the BHandHLYP/6-31G* level (shifted by 7146 cm^{-1}).

Table S4 TD-DFT calculated electronic and magnetic transition dipole moments, the angle ϑ, calculated rotatory strength R_{theo} and anisotropy factors g_{theo} of **(*R*)-mSQA**, **(*R*)-mSQB** and **(*R*)-mMC**.

	$\tilde{\nu}_{max}$ / cm^{-1}	$\lvert\boldsymbol{\mu}\rvert^c$ / esu·cm (/ D)	$\lvert\boldsymbol{m}\rvert$ / erg·G^{-1} (/ μ_B)	ϑ ($\boldsymbol{\mu}$,$\boldsymbol{m}$) / deg	R_{theo} / 10^{-40} cgs (/ D·μ_B)	$\lvert g_{theo}\rvert$ / cgs[d]
(*R*)-mSQA	15100	1.21 × 10^{-17} (12.1)	6.49 × 10^{-21} (0.70)	95.2	71.0 (0.77)	1.9 × 10^{-4}
	21800	2.90 × 10^{-19} (0.29)	5.00 × 10^{-21} (0.54)	21.2	–13.5 (–0.15)	6.4 × 10^{-2}
	33200	5.12 × 10^{-19} (0.51)	1.44 × 10^{-20} (1.55)	43.1	–53.7 (–0.58)	8.2 × 10^{-2}
(*R*)-mSQB	14000	9.83 × 10^{-18} (9.83)	1.26 × 10^{-20} (1.36)	88.6	–29.9 (–0.32)	1.2 × 10^{-4}
	24000	6.78 × 10^{-18} (6.78)	1.93 × 10^{-20} (2.08)	88.6	–31.0 (–0.34)	2.6 × 10^{-4}
	28100	3.73 × 10^{-18} (3.73)	2.32 × 10^{-21} (0.25)	116.8	38.9 (4.20)	1.1 × 10^{-3}
(*R*)-mMC	20200	9.41 × 10^{-18} (9.41)	9.24 × 10^{-21} (0.10)	89.3	–10.5 (–0.11)	4.8 × 10^{-5}
	21300	2.89 × 10^{-19} (0.29)	5.90 × 10^{-21} (0.64)	34.0	–14.1 (–0.15)	6.8 × 10^{-2}

Table S5 TD-DFT calculated values of $\boldsymbol{\mu}$, $\boldsymbol{m}$ in various units and the derived rotational strengths R_{theo} and anisotropy factors g_{theo} of **(*P*)-dSQA**.

$\tilde{\nu}_{max}$ / cm^{-1}		$\boldsymbol{\mu}$ / a.u[a]	$\boldsymbol{\mu}$ / *D* = 10^{-18} esu cm[b]	$\lvert\boldsymbol{\mu}\rvert$ / *D* = 10^{-18} esu cm[c]	$\boldsymbol{m}$ / a.u. = μ_B	$\boldsymbol{m}$ /10^{-20} erg·G^{-1} [d]	$\lvert\boldsymbol{m}\rvert$ / a.u. = μ_B	$\lvert\boldsymbol{m}\rvert$ / 10^{-20} erg G^{-1} [e]	R_{theo} / 10^{-40} cgs	R_{theo} / D μ_B	$\lvert g_{theo}\rvert$ / cgs[f]
14800	x	2.5608	6.5133	14.445	–3.6462	–3.3815	3.6538	3.3885	2484	26.8	4.8×10^{-3}
	y	5.0693	12.894		–0.2356	–0.2185					
	z	0.0000	0.0000		0.0000	0.0000					
15900	x	0.0000	0.0000	10.470	0.0000	0.0000	2.2559	2.0921	–2190	–23.6	8.0×10^{-3}
	y	0.0000	0.0000		0.0000	0.0000					
	z	–4.1163	–10.470		–2.2559	–2.0921					

[a] $\boldsymbol{\mu} = \boldsymbol{\mu}_{dip} = \boldsymbol{\mu}_{vel} / E$; [b] 1 a.u. = 2.5425 D., 1 D = 10^{-18} esu·cm; [c] $|\boldsymbol{\mu}| = \sqrt{\boldsymbol{\mu}_x^2 + \boldsymbol{\mu}_y^2 + \boldsymbol{\mu}_z^2}$; [d] 1 a.u. = 0.9274 erg·G^{-1}; [e] $|\boldsymbol{m}| = \sqrt{\boldsymbol{m}_x^2 + \boldsymbol{m}_y^2 + \boldsymbol{m}_z^2}$; [f] $g_{theo} = 4R_{theo}/\boldsymbol{\mu}^2$.

Table S6 TD-DFT calculated values of $\boldsymbol{\mu}$, $\boldsymbol{m}$ in various units and the derived rotational strengths R_{theo} and anisotropy factors g_{theo} of **(*P*)-dSQB**.

$\tilde{\nu}_{max}$ / cm^{-1}		$\boldsymbol{\mu}$ / a.u[a]	$\boldsymbol{\mu}$ / *D* = 10^{-18} esu cm[b]	$\lvert\boldsymbol{\mu}\rvert$ / *D* = 10^{-18} esu cm[c]	$\boldsymbol{m}$ / a.u. = μ_B	$\boldsymbol{m}$ /10^{-20} erg G^{-1} [d]	$\lvert\boldsymbol{m}\rvert$ / a.u. = μ_B	$\lvert\boldsymbol{m}\rvert$ / 10^{-20} erg G^{-1} [e]	R_{theo} / 10^{-40} cgs	R_{theo} / D μ_B	$\lvert g_{theo}\rvert$ / cgs[f]
13700	x	1.7693	4.5003	12.209	–2.5229	–2.3397	3.0489	2.8275	2855	30.8	7.7×10^{-3}
	y	–4.4619	–11.349		1.7119	1.5876					
	z	0.0000	0.0000		0.0000	0.0000					
14400	x	0.0000	0.0000	8.0189	0.0000	0.0000	3.4810	3.2283	–2589	–27.9	1.6×10^{-2}
	y	0.0000	0.0000		0.0000	0.0000					
	z	3.1527	8.0189		3.4819	3.2283					
24000	x	–1.0476	–2.6645	7.7527	2.7452	2.5459	3.5253	3.2694	2172	23.4	1.4×10^{-2}
	y	2.8624	7.2804		–2.2117	–2.0511					
	z	0.0000	0.0000		0.0000	0.0000					
24300	x	0.0000	0.0000	5.5383	0.0000	0.0000	4.6649	4.3263	–2396	–25.8	3.1×10^{-2}

	y	0.0000	0.0000		0.0000	0.0000					
	z	–2.1774	–5.5383		–4.6649	–4.3263					

[a] $\boldsymbol{\mu} = \boldsymbol{\mu}_{dip} = \boldsymbol{\mu}_{vel} / E$; [b] 1 a.u. = 2.5425 D., 1 D = 10^{-18} esu cm; [c] $|\boldsymbol{\mu}| = \sqrt{\boldsymbol{\mu}_x^2 + \boldsymbol{\mu}_y^2 + \boldsymbol{\mu}_z^2}$; [d] 1 a.u. = 0.9274 erg G^{-1}; [e] $|\boldsymbol{m}| = \sqrt{\boldsymbol{m}_x^2 + \boldsymbol{m}_y^2 + \boldsymbol{m}_z^2}$; [f] $g_{theo} = 4R_{theo}/\boldsymbol{\mu}^2$.

Table S7 TD-DFT calculated values of $\boldsymbol{\mu}$, $\boldsymbol{m}$ in various units and the derived rotational strengths R_{theo} and anisotropy factors g_{theo} of **(*P*)-dMC**.

$\tilde{\nu}_{max}$ / cm^{-1}		$\boldsymbol{\mu}$ / a.u[a]	$\boldsymbol{\mu}$ / *D* = 10^{-18} esu cm[b]	$\lvert\boldsymbol{\mu}\rvert$ / *D* = 10^{-18} esu cm[c]	$\boldsymbol{m}$ / a.u. = μ_B	$\boldsymbol{m}$ /10^{-20} erg G^{-1} [d]	$\lvert\boldsymbol{m}\rvert$ / a.u. = μ_B [e]	$\lvert\boldsymbol{m}\rvert$ / 10^{-20} erg G^{-1}	R_{theo} / 10^{-40} cgs	R_{theo} / D μ_B	$\lvert g_{theo}\rvert$ / cgs[f]
	x	–2.6375	–6.7086		4.1832	3.8800					
19700	y	–3.4681	–3.4681	11.082	–0.5572	–0.5167	4.2201	3.9138	2147	23.1	7.0×10^{-3}
	z	0.0000	0.0000		0.0000	0.0000					
	x	0.0000	0.0000		0.0000	0.0000					
20700	y	0.0000	0.0000	8.2801	0.0000	0.0000	2.7535	2.5536	–2114	–22.8	1.2×10^{-2}
	z	–3.2554	–8.2801		–2.7535	–2.5536					

[a] $\boldsymbol{\mu} = \boldsymbol{\mu}_{dip} = \boldsymbol{\mu}_{vel} / E$; [b] 1 a.u. = 2.5425 D., 1 D = 10^{-18} esu cm; [c] $|\boldsymbol{\mu}| = \sqrt{\boldsymbol{\mu}_x^2 + \boldsymbol{\mu}_y^2 + \boldsymbol{\mu}_z^2}$; [d] 1 a.u. = 0.9274 erg G^{-1}; [e] $|\boldsymbol{m}| = \sqrt{\boldsymbol{m}_x^2 + \boldsymbol{m}_y^2 + \boldsymbol{m}_z^2}$; [f] $g_{theo} = 4R_{theo}/\boldsymbol{\mu}^2$.

Table S8 TD-DFT calculated values of $\boldsymbol{\mu}$ and $\boldsymbol{m}$ of the monomeric subunits in the dimer (***P***)-**dSQA**, and the derived rotational strengths R_{mon}, $R_{e\text{-}m}$ and R_{ex}.

		$\boldsymbol{\mu}$ / a.u.[a]	$\boldsymbol{\mu}$ / D =10^{-18} esu cm[b]	$\lvert\boldsymbol{\mu}\rvert$ / D = 10^{-18} esu cm[c]	$\boldsymbol{m}$ / a.u. = μ_B	$\boldsymbol{m}$ / 10^{-20} erg G^{-1}[d]	$\lvert\boldsymbol{m}\rvert$ / a.u. = μ_B[e]	$\lvert\boldsymbol{m}\rvert$ / 10^{-20} erg G^{-1}		$\boldsymbol{r}_{21}$ / Å	λ / Å	R_{mon} / 10^{-40} cgs[f]	R_{mon} / D·μ_B	$R_{e\text{-}m}$ / 10^{-40} cgs[g]	$R_{e\text{-}m}$ / D·μ_B	R_{ex} / 10^{-40} cgs[h]	R_{ex} / D μ_B[i]
	x	0.2109	0.5363		0.3387	0.3141											
Mon1	y	4.5928	11.682	12.108	0.0821	0.0762	0.7000	0.6492									
	z	1.2344	3.1396		–0.6071	–0.5631											
	x	–2.2986	–5.8466		–0.5089	–0.4720											
Mon2	y	0.2018	0.5132	12.108	0.3090	–0.2866	0.7000	0.6492									
	z	–4.1639	–10.591		0.3682	–0.3415											
									x	0.1108							
									y	5.9238	5115.7	71.0	0.77	±417	±4.49	±1752	±19.1
									z	9.6163							

[a] $\boldsymbol{\mu} = \boldsymbol{\mu}_{dip} = \boldsymbol{\mu}_{vel} / E$; [b] 1 a.u. = 2.5425 D., 1 D = 10^{-18} esu cm; [c] $|\boldsymbol{\mu}| = \sqrt{\boldsymbol{\mu}_x^2 + \boldsymbol{\mu}_y^2 + \boldsymbol{\mu}_z^2}$; [d] 1 a.u. = 0.9274 erg G^{-1}; [e] $|\boldsymbol{m}| = \sqrt{\boldsymbol{m}_x^2 + \boldsymbol{m}_y^2 + \boldsymbol{m}_z^2}$; [f] $R_{mon} = -(\boldsymbol{\mu}_1 \cdot \boldsymbol{m}_1 + \boldsymbol{\mu}_2 \cdot \boldsymbol{m}_2)$; [g] $R_{e\text{-}m} = -(\boldsymbol{\mu}_1 \cdot \boldsymbol{m}_2 + \boldsymbol{\mu}_2 \cdot \boldsymbol{m}_1)$; [h] R_{ex} [cgs] $= -(\pi/2\lambda)\, \boldsymbol{r}_{21} (\boldsymbol{\mu}_1 \times \boldsymbol{\mu}_2)$; [i] R_{ex} [D μ_B] $= -(171/\lambda)\, \boldsymbol{r}_{21} (\boldsymbol{\mu}_1 \times \boldsymbol{\mu}_2)$.

Table S9 TD-DFT calculated values of $\boldsymbol{\mu}$ and $\boldsymbol{m}$ of the monomeric subunits in the dimer (***P***)-**dSQB**, and the derived rotational strengths R_{mon}, $R_{e\text{-}m}$ and R_{ex}.

		$\boldsymbol{\mu}$ / a.u.[a]	$\boldsymbol{\mu}$ / D =10^{-18} esu cm[b]	$\lvert\boldsymbol{\mu}\rvert$ / D = 10^{-18} esu cm[c]	$\boldsymbol{m}$ / a.u. = μ_B	$\boldsymbol{m}$ / 10^{-20} erg G^{-1}[d]	$\lvert\boldsymbol{m}\rvert$ / a.u. = μ_B[e]	$\lvert\boldsymbol{m}\rvert$ / 10^{-20} erg G^{-1}		$\boldsymbol{r}_{21}$ / Å	λ / Å	R_{mon} / 10^{-40} cgs[f]	R_{mon} / D·μ_B	$R_{e\text{-}m}$ / 10^{-40} cgs[g]	$R_{e\text{-}m}$ / D·μ_B	R_{ex} / 10^{-40} cgs[h]	R_{ex} / D μ_B[i]
	x	–1.0299	–2.6197		0.3579	0.3320											
Mon1	y	–3.6211	–9.2103	9.8323	–0.4360	–0.4043	1.3571	1.2586									
	z	–0.8777	–2.2323		1.2344	1.1447											
	x	2.6147	6.6505		0.3375	0.3130											
Mon2	y	–0.2437	–0.6198	9.8323	–1.2600	–1.1685	1.3571	1.2586									
	z	2.8368	7.2153		–0.3747	–0.3475											
									x	1.0852							
									y	5.1466	5719.0	–29.9	–0.32	±1071	±11.6	±1457	±15.9
									z	9.2751							

[a] $\boldsymbol{\mu} = \boldsymbol{\mu}_{dip} = \boldsymbol{\mu}_{vel} / E$; [b] 1 a.u. = 2.5425 D., 1 D = 10^{-18} esu cm; [c] $|\boldsymbol{\mu}| = \sqrt{\boldsymbol{\mu}_x^2 + \boldsymbol{\mu}_y^2 + \boldsymbol{\mu}_z^2}$; [d] 1 a.u. = 0.9274 erg G^{-1}; [e] $|\boldsymbol{m}| = \sqrt{\boldsymbol{m}_x^2 + \boldsymbol{m}_y^2 + \boldsymbol{m}_z^2}$; [f] $R_{mon} = -(\boldsymbol{\mu}_1 \cdot \boldsymbol{m}_1 + \boldsymbol{\mu}_2 \cdot \boldsymbol{m}_2)$; [g] $R_{e\text{-}m} = -(\boldsymbol{\mu}_1 \cdot \boldsymbol{m}_2 + \boldsymbol{\mu}_2 \cdot \boldsymbol{m}_1)$; [h] R_{ex} [cgs] $= -(\pi/2\lambda)\, \boldsymbol{r}_{21} (\boldsymbol{\mu}_1 \times \boldsymbol{\mu}_2)$; [i] R_{ex} [D μ_B] $= -(171/\lambda)\, \boldsymbol{r}_{21} (\boldsymbol{\mu}_1 \times \boldsymbol{\mu}_2)$.

Table S10 TD-DFT calculated values of $\boldsymbol{\mu}$ and $\boldsymbol{m}$ of the monomeric subunits in the dimer **(*P*)-dMC**, and the derived rotational strengths R_{mon}, $R_{e\text{-}m}$ and R_{ex}.

		$\boldsymbol{\mu}$ / a.u.[a]	$\boldsymbol{\mu}$ / *D* $=10^{-18}$ esu cm[b]	$\lvert\boldsymbol{\mu}\rvert$ / D = 10^{-18} esu cm[c]	$\boldsymbol{m}$ / a.u. = μ_B	$\boldsymbol{m}$ / 10^{-20} erg G^{-1}[d]	$\lvert\boldsymbol{m}\rvert$ / a.u. = μ_B[e]	$\lvert\boldsymbol{m}\rvert$ / 10^{-20} erg G^{-1}	$\boldsymbol{r}_{21}$ / Å		λ / Å	R_{mon} / 10^{-40} cgs[f]	R_{mon} / D·μ_B	$R_{e\text{-}m}$ / 10^{-40} cgs[g]	$R_{e\text{-}m}$ / D·μ_B	R_{ex} / 10^{-40} cgs[h]	R_{ex} / D μ_B[i]
Mon1	x	–0.3040	–0.7732	9.4064	0.1998	0.1853	0.9964	0.9240	x	–0.3833	3657.1	–10.6	–0.11	±826	±8.91	±1227	±12.3
	y	–3.5380	–8.9988		–0.3009	–0.2791			y	5.2314							
	z	–1.0331	–2.6276		0.9286	0.8612			z	8.2972							
Mon2	x	1.4040	3.5710	9.4064	0.1792	0.1662	0.9964	0.9240									
	y	–0.1632	–0.4151		–0.9742	–0.9035											
	z	3.4175	8.6923		–0.1071	–0.0993											

[a] $\boldsymbol{\mu} = \boldsymbol{\mu}_{dip} = \boldsymbol{\mu}_{vel} / E$; [b] 1 a.u. = 2.5425 D., 1 D = 10^{-18} esu cm; [c] $|\boldsymbol{\mu}| = \sqrt{\boldsymbol{\mu}_x^2 + \boldsymbol{\mu}_y^2 + \boldsymbol{\mu}_z^2}$; [d] 1 a.u. = 0.9274 erg G^{-1}; [e] $|\boldsymbol{m}| = \sqrt{\boldsymbol{m}_x^2 + \boldsymbol{m}_y^2 + \boldsymbol{m}_z^2}$; [f] $R_{mon} = -(\boldsymbol{\mu}_1 \cdot \boldsymbol{m}_1 + \boldsymbol{\mu}_2 \cdot \boldsymbol{m}_2)$; [g] $R_{e\text{-}m} = -(\boldsymbol{\mu_1} \cdot \boldsymbol{m_2} + \boldsymbol{\mu_2} \cdot \boldsymbol{m_1})$; [h] R_{ex} [cgs] $= -(\pi/2\lambda)\, \boldsymbol{r}_{21}\, (\boldsymbol{\mu_1} \times \boldsymbol{\mu_2})$; [i] R_{ex} [D μ_B] $= -(171/\lambda)\, \boldsymbol{r}_{21}\, (\boldsymbol{\mu_1} \times \boldsymbol{\mu_2})$.

5 Chromatograms

All chromatograms of mixtures of diastereomers were obtained by repeating the reactions with racemic mixtures instead of enantiopure compounds.

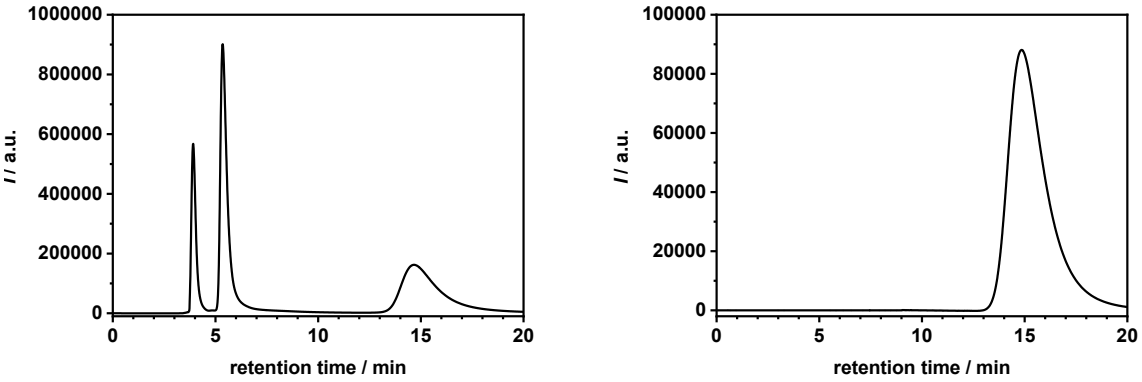

Fig. S14 Chromatograms of **dSQA**. Left: mixture of stereoisomers, right: **(*P*)-dSQA** (RR).

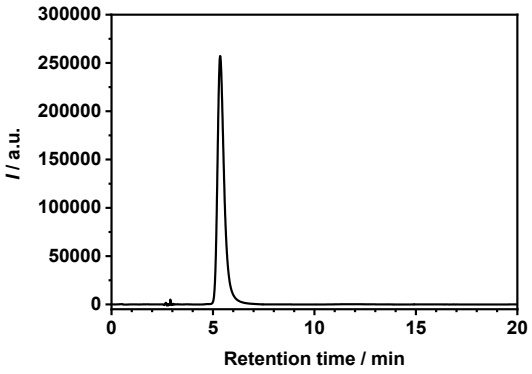

Fig. S15 Chromatogram of **(*M*)-dSQA** (SS).

Table S11 Data obtained from analytical HPLC of **dSQA**.

LUX Amylose-3; THF/hexane 9:1; 1 mL/min; detection at 715 nm; t(1) = 3.9 min; t(2) = 5.3 min; t(3) = 14.7 min								
	Area 1	Area 2	Area 3	%1	%2	%3	%ee	%de
Mixture (RR, RS, SS)	152773	381943	354371	17.2	43.0	39.8	-	-
RR	0	17	191769	< 0.1	< 0.1	> 99.9	> 99.9	100
SS	23	100965	116	< 0.1	99.9	0.1	99.8	> 99.9

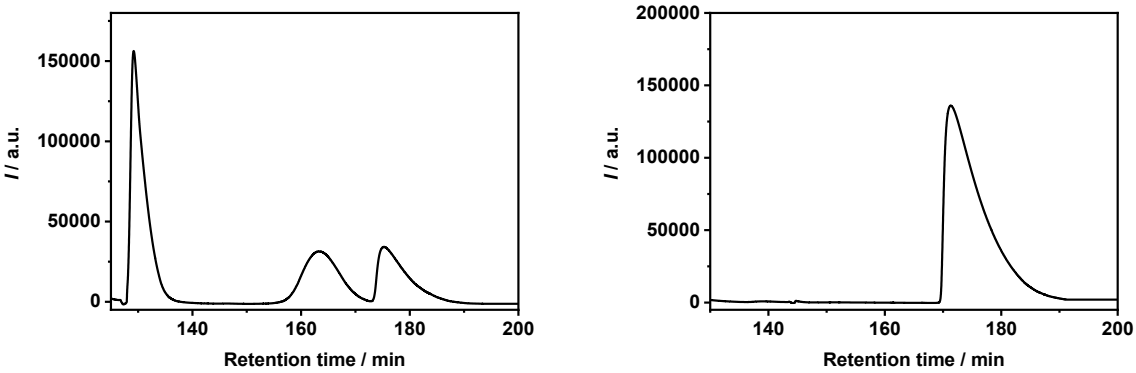

Fig. S16 Chromatograms of **dSQB**. Left: mixture of stereoisomers, right: **(*P*)-dSQB** (RR).

Table S12 Data obtained from analytical HPLC of **(*P*)-dSQB**.

LUX Amylose-3; Hexane/DCM/iPrOH 120:40:3; 1 mL/min; detection at 715 nm; t(1) = 129.2 min; t(2) = 163.4 min; t(3) = 175.3 min								
	Area 1	Area 2	Area 3	%1	%2	%3	%ee	%de
Mixture (RR, RS, SS)	464290	240478	206366	51.0	26.4	22.6	-	
RR	1512	3762	1024188	0.1	0.4	99.5	99.2	99.9

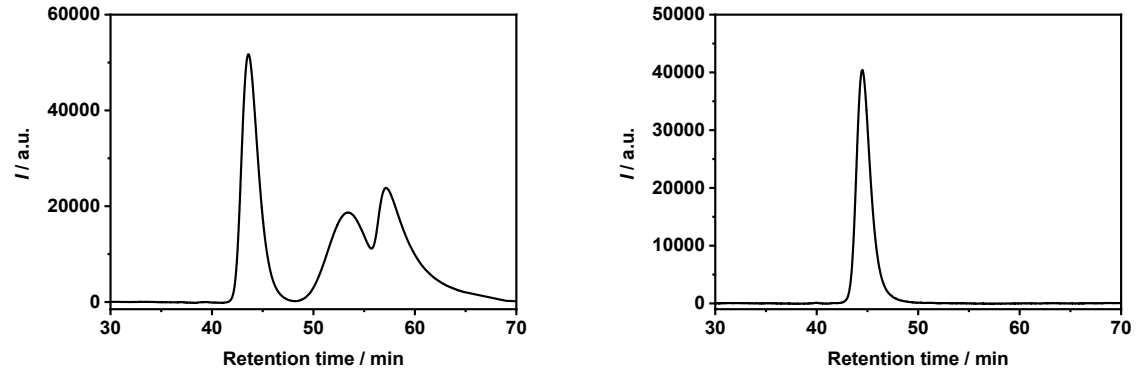

Fig. S17 Chromatograms of **dSQB**. Left: mixture of stereoisomers, right: **(*M*)-dSQB** (SS).

Table S13 Data obtained from analytical HPLC of **(*M*)-dSQB**.

LUX Amylose-3; Hexane/DCM/iPrOH 120:50:10; 1 mL/min; detection at 715 nm; t(1) = 43.5 min; t(2) = 53.4 min; t(3) = 57.2 min						
	Area 1	Area 2	%1	%2	%ee	%de
Mixture (RR, RS, SS)	104461	180187	36.7	63.3	-	
SS	69846	157	99.8	0.2	> 99.6	> 99.6

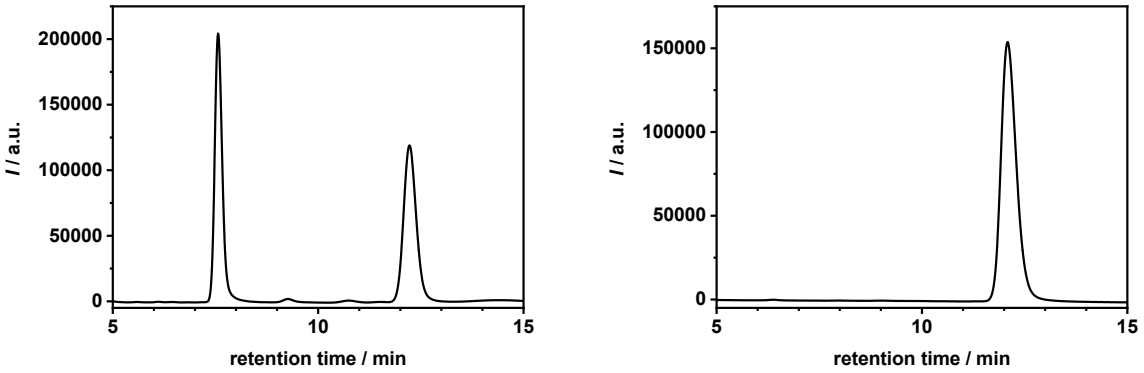

Fig. S18 Chromatograms of **5**. Left: mixture of stereoisomers, right: **(*R*)-5**.

Table S14 Data obtained from analytical HPLC of **5**.

LUX Cellulose-4; Hexane/iPrOH 9:1; 1 mL/min; detection at 254 nm; t(1) = 7.6 min; t(2) = 12.2 min					
	Area 1	Area 2	%1	%2	%ee
Mixture (R & S)	41893	40636	50.8	49.2	-
R	10	64121	0.1	99.9	99.8

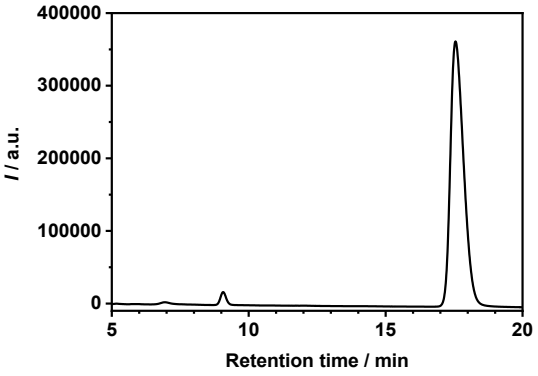

Fig. S19 Chromatogram of **15**.

The chromatogram of the racemic mixture can be found in literature.[3]

Table S15 Data obtained from analytical HPLC of **15**.

LUX Cellulose-4; Hexane/iPrOH 9:1; 1 mL/min; detection at 254 nm; t(1) = 9.1 min; t(2) = 17.6 min				
Area 1	Area 2	%1	%2	%ee
3107	197465	1.5	98.5	97.0

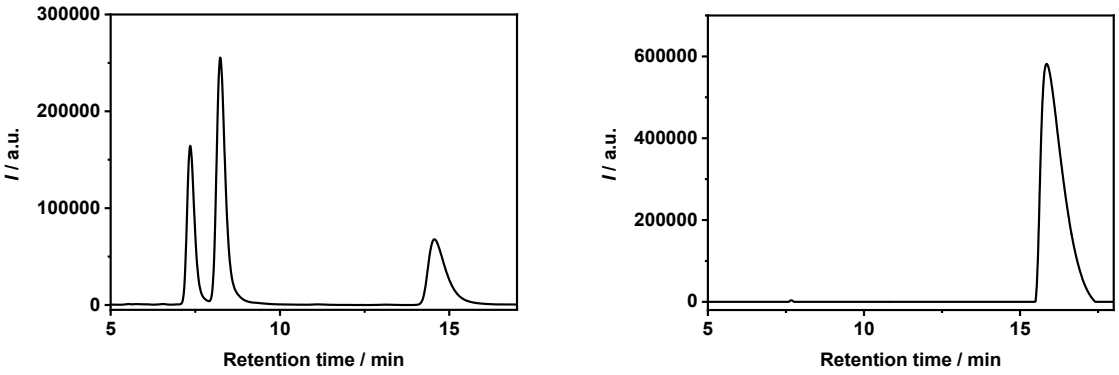

Fig. S20 Chromatogram of **8**. Left: mixture of stereoisomers, right: (***P***)-**8**.

	LUX Amylose-3; Hexane/THF 4:1; 1 mL/min; detection at 254 nm; t(1) = 7.4 min; t(2) = 8.2 min; t(3) = 14.6 min							
	Area 1	Area 2	Area 3	%1	%2	%3	%ee	%de
Mixture (RR, RS, SS)	44355	82696	42571	26.1	48.8	25.1	-	-
RR	402	0	474984	0.1	0	99.9	99.8	100

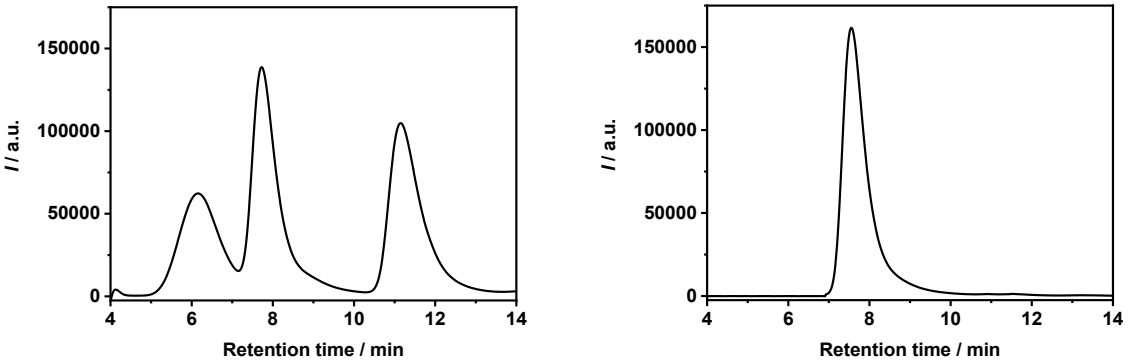

Fig. S21 Chromatogram of **dMC**. Left: mixture of stereoisomers, right: (***P***)**-dMC** (RR).

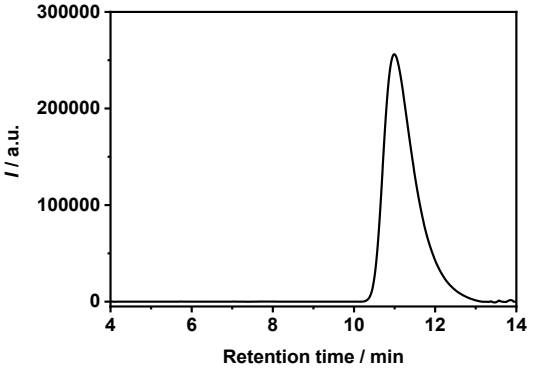

Fig. S22 Chromatogram: (***M***)**-dMC** (SS).

LUX Amylose-3; Toluene/THF 98:2; 1 mL/min; detection at 505 nm; t(1) = 6.2 min; t(2) = 7.7 min; t(3) = 11.1 min								
	Area 1	Area 2	Area 3	%1	%2	%3	%ee	%de
Mixture (RR, RS, SS)	72350	108581	103294	25.5	38.2	36.3	-	-
RR	0	119151	572	0	99.5	0.5	99.0	100
SS	6	18	236166	< 0.1	< 0.1	> 99.9	> 99.9	> 99.9

6 Self-absorption correction of the CPL spectra

Following equations were used for the self-absorption correction:[4, 5]

$$Fl_{\text{corr}} = \frac{Fl_{\text{obs}}}{T} \tag{S6}$$

$$CPL_{corr} = \frac{Fl_{obs}\,\alpha \ln(10)\,\Delta OD}{T} + \frac{CPL_{obs}}{T} = CD\ \text{Term} + CPL\ \text{Term} \tag{S7}$$

$$g_{lum,\,corr} = \frac{CPL_{corr}}{Fl_{corr}} = \alpha \ln(10)\,\Delta OD \frac{CPL_{obs}}{Fl_{obs}} = \alpha \ln(10)\,\Delta OD g_{lum,\,obs} \tag{S8}$$

7 Synthesis

All reactions were carried out in standard glass ware. All chemicals were purchased from commercial suppliers and were used without further purification. For reactions performed under nitrogen atmosphere standard Schlenk techniques were used. Nitrogen was dried over Sicapent® from Merck and oxygen was removed via copper catalyst R3-11 from BASF. Solvents, if not taken from the SPS, were dried according to standard literature procedures and stored under inert gas atmosphere. Column chromatography and thin layer chromatography were performed on silica gel (40 – 63 µm, Macherey-Nagel) in wet-packed glass columns and TLC plates (Macherey-Nagel), respectively.

Synthesis of compounds **2**, **3**, **10**, **14**, **15** was done according to literature.[3, 6, 7]

To avoid the enantioselective synthesis of (*S*)-oxindole **7**, the (*M*)-enantiomers of all dimeric dyes were either obtained by separation of a racemic dye mixture prepared from racemic oxindole **7** or by separation of the (*M*)-enantiomer of bis-oxindole **8** by preparative HPLC on a chiral phase.

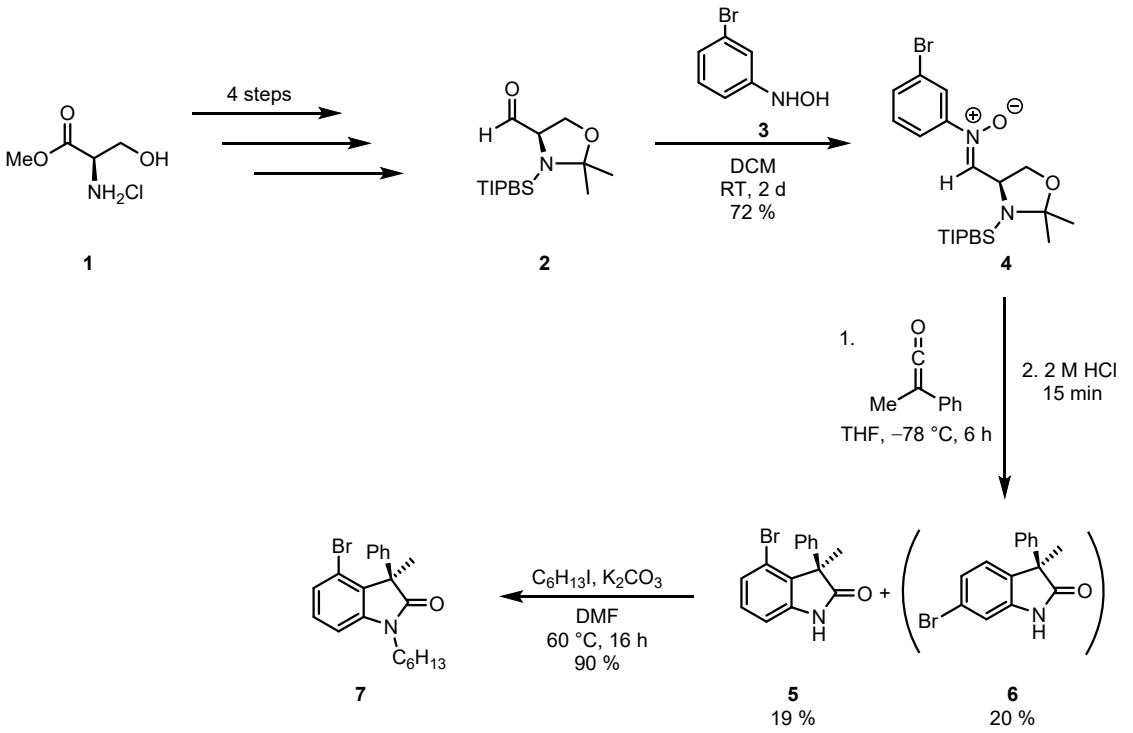

Fig. S23 Synthesis of chiral oxindole **7** via a pericyclic cascade reaction. Compound **6** was a byproduct of the synthesis of **5** and not further used.

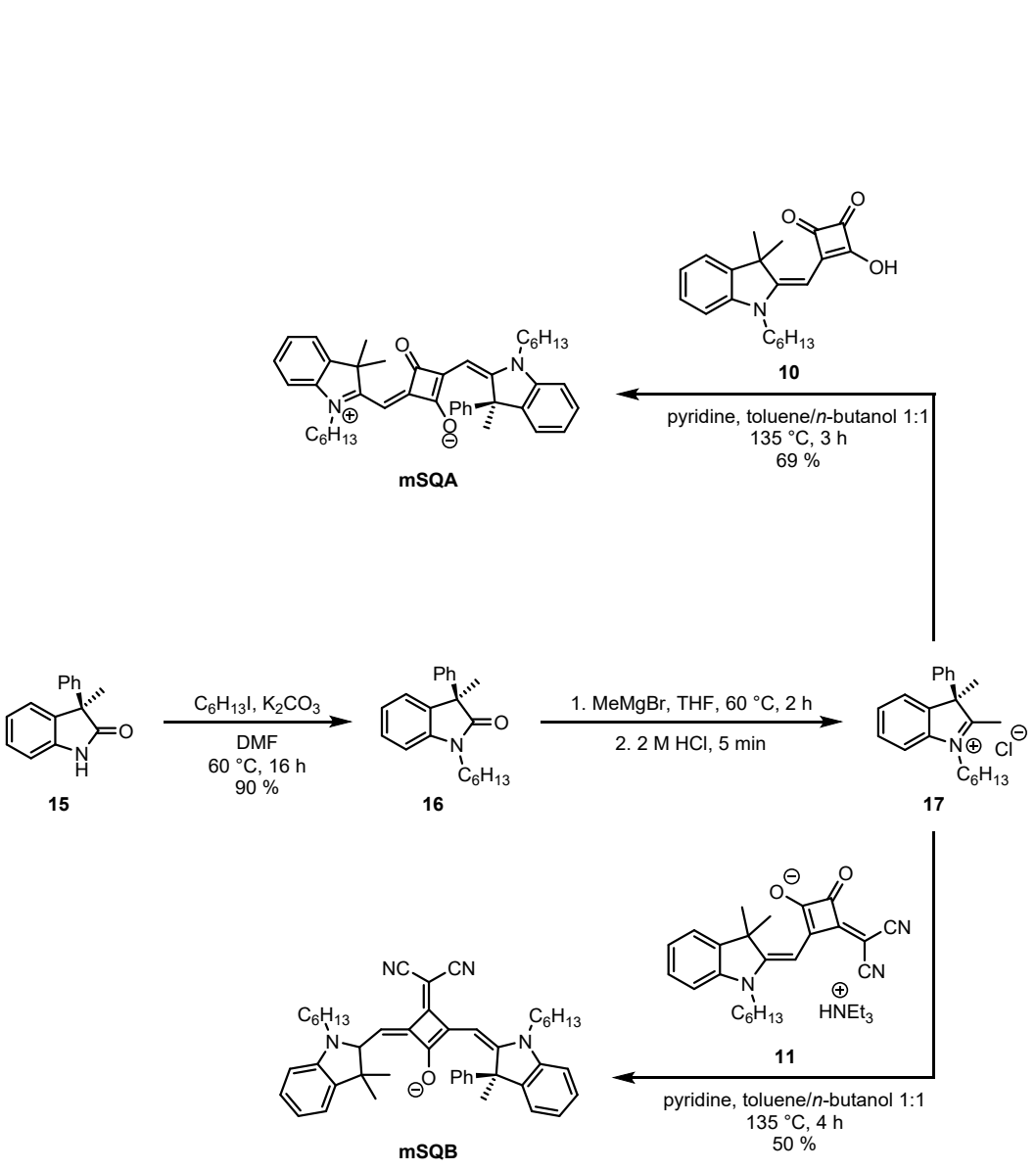

Fig. S24 Synthesis of compound **11**.

Fig. S25 Synthesis of **mSQA** and **mSQB**.

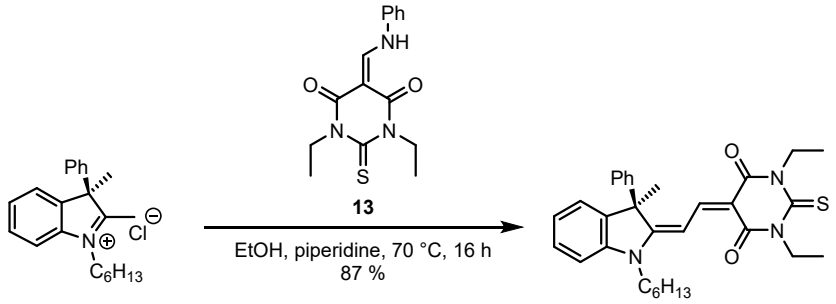

Fig. S26 Synthesis of **mMC**.

Synthesis of compound 16

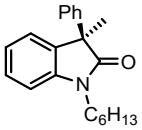

Following a synthetic protocol reported in the literature,[8] compound **15** (145 mg, 649 µmol) and oven-dried K_2CO_3 (898 mg, 6.50 mmol) were suspended in dry DMF (5 mL) under a nitrogen atmosphere and stirred at RT for 30 min. 1-Iodohexane (331 mg, 1.56 mmol) was added and the mixture was stirred at 60 °C for 16 h. After cooling, H_2O (4 mL) was added and the aqueous phase was extracted with DCM (3 × 5 mL). The combined organic phases were dried over $MgSO_4$ and the solvent was removed *in vacuo*. The crude product was purified by flash column chromatography (SiO_2, eluent: PE/EA 20:1).

Yield: 180 mg (585 µmol, 90 %) of a colourless solid.

$C_{21}H_{25}NO$ [307.4443]

^{1}H NMR (400 MHz, CD_2Cl_2, 295 K)

δ [ppm]: 7.23 – 7.15 (m‘, 6H, 5 × Ph*H* & -C*H*-), 7.05 (dd, 1H, $^3J_{HH}$ = 7.4 Hz, $^4J_{HH}$ = 1.4 Hz, -C*H*-), 6.97 (dd, 1H, $^3J_{HH}$ = 7.4 Hz, $^4J_{HH}$ = 1.0 Hz, -C*H*-), 6.87 (d, 1H, $^3J_{HH}$ = 7.8 Hz, -C*H*-), 3.70 – 3.56 (m, 2H, -NCH_2-), 1.66 (s, 3H, -CH_3), 1.63 – 1.57 (m, 2H, -NCH$_2$CH_2-), 1.28 – 1.19 (m, 6H, -CH_2-), 0.80 – 0.76 (m, 3H, -CH$_2$CH_3).

^{13}C NMR (101 MHz, CD_2Cl_2, 295 K)

δ [ppm]: 179.5 (quart.), 142.8 (quart.), 141.1 (quart.), 135.3 (quart.), 128.7 (tert.), 128.1 (tert.), 127.3 (tert.), 126.7 (tert.), 124.4 (tert.), 122.6 (tert.), 108.7 (tert.), 52.2 (quart.), 40.2 (sec.), 31.5 (sec.), 27.5 (sec.), 26.6 (sec.), 23.8 (prim.), 22.6 (sec.), 14.1 (prim.).

Synthesis of compound 4

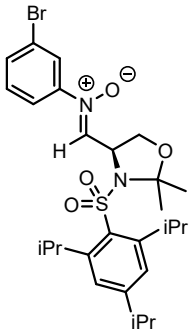

Following a synthetic protocol reported in the literature,[3] compound **2** (3.30 g, 8.34 mmol) was dissolved in DCM (30 mL) and $MgSO_4$ (1.10 g, 9.14 mmol) was added. The mixture was stirred at rt for 5 min. Then, **3** (2.04 g, 10.8 mmol) was added stirred at rt for 2 d. After filtration of the $MgSO_4$, the solvent was removed *in vacuo*. The crude product was purified by column chromatography (SiO_2, eluent: PE/acetone 9:1).

Yield: 3.40 g (6.01 mmol, 72 %) of a yellow oil.$C_{27}H_{37}BrN_2O_4S$ [565.56]

^{1}H NMR (400 MHz, CD_2Cl_2, 295 K)

δ [ppm]: 7.52 (ddd, 1H, $^3J_{HH}$ = 8.0 Hz, $^4J_{HH}$ = 1.9 Hz, $^4J_{HH}$ = 0.9 Hz, -C*H*-), 7.38 (dd, 1H, $^4J_{HH}$ = 2.1 Hz, $^4J_{HH}$ = 1.9 Hz, -C*H*-), 7.17 (dd, 1H, $^3J_{HH}$ = 8.1 Hz, $^3J_{HH}$ = 8.0 Hz, -C*H*-), 6.89 (ddd, 1H, $^3J_{HH}$ = 8.1 Hz, $^4J_{HH}$ = 2.1 Hz, $^4J_{HH}$ = 0.9 Hz, -C*H*-), 6.70 (d, 1H, $^3J_{HH}$ = 5.3 Hz, -*H*CN$^+$-), 5.05 – 5.02 (m, 1H, -C*H*N-), 4.43 (dd, 1H, $^2J_{HH}$ = 9.5 Hz, $^3J_{HH}$ = 7.3 Hz, 1 × -CH_2-), 4.36 – 4.29 (m, 2H, *o*-iPr*H*), 4.15 (dd, 1H, $^2J_{HH}$ = 9.5 Hz, $^3J_{HH}$ = 2.1 Hz, 1 × -CH_2-), 2.87 (sep, 1H, $^3J_{HH}$ = 6.9 Hz,

p-iPr*H*), 1.80 (s, 3H, -CCH_3), 1.79 (s, 3H, -CCH_3), 1.27 – 1.15 (m‘, 18H, 6 × iPrCH_3).

^{13}C NMR (101 MHz, CD_2Cl_2, 295 K)

δ [ppm]: 154.8 (quart.), 152.0 (quart.), 147.6 (quart.), 139.4 (tert.), 133.8 (tert.), 132.6 (quart.), 130.7 (tert.), 124.8 (2 * tert.), 122.9 (quart.), 119.7 (tert.), 100.5 (quart.), 68.2 (sec.), 56.3 (tert.), 34.5 (tert.), 29.5 (2 × tert.), 28.2 (prim.), 25.1 (prim.), 24.8 (prim.), 23.4 (prim.).

ESI-MS (pos.): $[C_{27}H_{37}BrN_2O_4S+Na]^{\cdot+}$

calcd.: 589.1532

exp.: 589.1527

Synthesis of compound 5

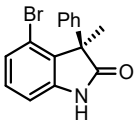

Following a synthetic protocol reported in the literature,[3] compound **4** (980 mg, 1.73 mmol) was dissolved in dry THF (10 mL) under a nitrogen atmosphere and cooled to -78 °C. Methylphenylketen (366 mg, 2.77 mmol) in dry THF (1 mL) was slowly added dropwise and the mixture was stirred at –78 °C for 6 h. HCl (2 mL, 2 M) was added, stirred for 30 min and allowed to warm up to rt. After extraction with diethyl ether (3 × 30 mL) the combined organic phases were washed with a saturated. $NaHCO_3$-solution dried over $MgSO_4$ and filtrated. The solvent was removed *in vacuo*. The crude product was purified by column chromatography (SiO_2, Laufmittel: PE/EA 9:1 → 4:1) and recrystallisation from MeCN/H_2O (1:1, 10 ml).

Yield: 100 mg (331 µmol, 19 %) of a colourless solid.

HPLC: 99 % ee, eluent: hexane/iPrOH: 9:1, retention times 8.2 min (minor, 0.1 %), 14.1 min (major, 99.9 %).

$C_{15}H_{12}BrNO$ [302.17]

^{1}H NMR (400 MHz, $CDCl_3$, 295 K)

δ [ppm]: 8.24 (br s, 1H, -N*H*-), 7.34 – 7.27 (m‘, 3H, Ph*H*), 7.23 – 7.19 (m’ 2H, Ph*H*), 7.18 (dd, 1H, $^3J_{HH}$ = 8.2 Hz, $^4J_{HH}$ = 1.2 Hz, -C*H*-), 7.13 (dd, 1H, $^3J_{HH}$ = 8.2 Hz, $^3J_{HH}$ = 7.5 Hz, -C*H*-), 6.92 (dd, 1H, $^3J_{HH}$ = 7.5 Hz, $^4J_{HH}$ = 1.2 Hz, -C*H*-), 1.98 (s, 3H, -CH_3).

^{13}C NMR (101 MHz, $CDCl_3$, 295 K)

δ [ppm]: 180.7 (quart.), 142.5 (quart.), 137.9 (quart.), 133.9 (quart.), 129.8 (tert.), 128.7 (tert.), 127.6 (tert.), 127.2 (tert.), 126.9 (tert.), 120.0 (quart.), 109.1 (tert.), 54.5 (quart.), 19.8 (prim.).

ESI-MS (pos.): $[C_{15}H_{12}BrNO + Na]^+$

calcd.: 323.9994

exp.: 323.9992

Synthesis of compound 7

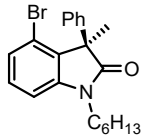

Following a synthetic protocol reported in the literature,[8] compound **6** (100 mg, 331 µmol) and oven-dried K_2CO_3 (457 mg, 3.31 mmol) were suspended in dry DMF (3 mL) under a nitrogen atmosphere and stirred at rt for 30 min. 1-Iodohexane (168 mg, 792 µmol) was added and the mixture was stirred at 60 °C for 16 h. After cooling, H_2O (3 mL) was added and the aqueous phase was extracted with DCM (3 × 5 mL). The combined organic phases were dried over $MgSO_4$ and the solvent was removed *in vacuo*. The crude product was purified by flash column chromatography (SiO_2, eluent: PE/EA 20:1).

Yield: 115 mg (298 µmol, 90 %) of a colourless solid.

$C_{21}H_{24}BrNO$ [386.33]

^{1}H NMR (400 MHz, CD_2Cl_2, 295 K)

δ [ppm]: 7.32 – 7.26 (m‘, 3H, Ph*H*), 7.21 (dd, 1H, $^3J_{HH}$ = 8.2 Hz, $^3J_{HH}$ = 7.5 Hz, -C*H*-), 7.18 – 7.14 (m‘, 3H, 2 × Ph*H* & 1 × -C*H*-), 6.93 (dd, 1H, $^3J_{HH}$ = 7.5 Hz, $^4J_{HH}$ = 1.2 Hz, -C*H*-), 3.75 – 3.62 (m, 2H, -NCH_2-), 1.90 (s, 3H, -CH_3), 1.68 – 1.64 (m, 2H, -NCH$_2$CH_2-), 1.33 – 1.26 (m’, 6H, 3 × -CH_2-), 0.85 (s, 3H, -CH$_2$CH_3).

^{13}C-NMR (101 MHz, CD_2Cl_2, 295 K)

δ [ppm]: 178.7 (quart.), 145.4 (quart.), 139.0 (2 × quart.), 133.9 (quart.), 130.0 (tert.), 128.8 (tert.), 127.6 (tert.), 127.1 (tert.), 126.8 (tert.), 119.9 (quart.), 108.0 (tert.), 40.6 (sec.), 31.8 (sec.), 27.6 (sec.), 26.8 (sec.), 22.9 (sec.), 19.7 (prim.), 14.1 (prim.).

ESI-MS (pos.): $[C_{21}H_{24}BrNO]^{\cdot+}$

calcd.: 387.1018

exp.: 387.1143

Synthesis of compound 11

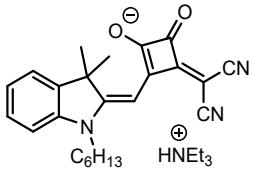

Following a synthetic protocol reported in the literature,[9] compound **14** (620 mg, 1.69 mmol) was dissolved in EtOH (37 ml). NEt_3 (1.65 ml, 11.8 mmol) and propanedinitrile (223 mg, 3.38 mmol) were added and the mixture was stirred at rt for 1 h. The solvent was removed in vacuo. The crude product was purified by flash column chromatography (SiO_2, eluent: DCM/MeOH 10:1).

Yield: 810 mg (1.66 mmol, 98 %) of a red solid.

$C_{30}H_{40}N_4O_2$ [488.67]

^{1}H-NMR (400 MHz, $CDCl_3$, 295 K)

δ [ppm]: 8.86 (br, 1H, *H*NEt_3), 7.32 (dd, 1H, ^3J = 7.3 Hz, ^4J = 0.9 Hz, -C*H*-), 7.22 – 7.18 (m, 1H, -C*H*-), 6.98 – 6.91 (m', 2H, -C*H*-), 5.91 (s, 1H, -CC*H*C-), 3.72 (t, 2H, ^3J = 7.5 Hz, -NCH_2CH_2-), 3.09 (q, 6H, ^3J = 7.2 Hz, 3 × -NCH_2CH_3), 1.62 – 1.57 (m, 2H, -NCH_2CH_2-), 1.56 (s, 6H, -C(CH_3)$_2$), 1.36 – 1.24 (m', 6H, 3 × -CH_2-), 1.17 (t, 9H, ^3J = 7.2 Hz, 3 × -NCH_2CH_3), 0.83 (t, 3H, ^3J = 7.1 Hz, -CH_2CH_3).

^{13}C-NMR (101 MHz, $CDCl_3$, 295 K)

δ [ppm]: 191.8 (2 × quart.), 185.3 (2 × quart.), 177.2 (2 × quart.), 167.5 (quart.), 162.7 (quart.), 143.0 (quart.), 140.1 (quart.), 127.6 (tert.), 121.8 (tert.), 120.9 (tert.), 107.8 (tert.), 84.2 (tert.), 46.4 (quart.), 45.8 (sec.), 42.1 (sec.), 31.0 (sec.) 27.1 (sec.), 25.9 (sec.), 25.7 (sec.), 22.0 (prim.), 13.9 (prim.), 8.7 (prim.).

ESI-MS (pos.): $[C_{24}H_{24}N_3O_2]^{\cdot+}$

calcd.: 386.1863

exp.: 386.1872

ESI-MS (pos.): $[C_{21}H_{25}NNaO_3]^{\cdot+}$

calcd.: 362.1727

exp.: 362.1725

Synthesis of (*R*)-mSQA

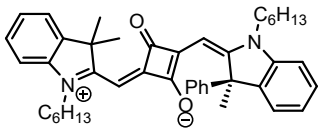

Following a synthetic protocol reported in the literature,[10] compound **16** (20.0 mg, 65.1 µmol) was dissolved in THF (1 ml) under a nitrogen atmosphere and a solution of MeMgBr in Et_2O (0.090 mL, 3.0 M, 270 µmol) was added. After stirring at 60 °C for 2 h, MeOH (0.2 ml) was added and the solvent was removed *in vacuo*. The residue was treated with an aqueous HCl solution (2 M, 1 ml) and extracted with DCM (3 × 10 ml). The combined organic phases were dried over $MgSO_4$ and the solvent was removed *in vacuo*. Due to the instability of the compound, the crude product **17** was used without further purification.

Compounds **17** (22.3 mg, 65.2 µmol) and **10** (26.5 mg, 78.1 µmol) were dissolved in a 1:1 mixture of toluene and 1-butanol (5 ml) and pyridine (0.35 ml). Using a Dean-Stark-trap, the mixture was stirred at 135 °C for 4 h. The solvent was removed *in vacuo*. The crude product was purified by flash column chromatography (SiO_2, eluent: DCM/MeOH 99.5:0.5 → 99:1) and precipitation from dichloromethane to hexane.

Yield: 28.0 mg (44.7 µmol, 69 %) of a blue solid.

$C_{43}H_{50}N_2O_2$ [626.87]

^{1}H-NMR (600 MHz, CD_2Cl_2, 295 K)

δ [ppm]: 7.34 (dd, 1H, $^{3}J_{HH}$ = 7.4 Hz, $^{4}J_{HH}$ = 0.6 Hz, -C*H*-), 7.30 (m‘, 3H, -C*H*-), 7.28 – 7.23 (m‘, 3H, Ph*H*), 7.18 – 7.10 (m‘, 3H, 1 × Ph*H* & 2 × -C*H*-), 7.04 – 7.00 (m‘, 3H, 1 × Ph*H* & 2 × -C*H*-), 6.02 (br s, 1H, -CC*H*C-), 5.76 (br s, 1H, -CC*H*C-), 4.14 – 3.90 (m‘, 4H, 2 × -NCH_2-), 2.26 – 2.15 (m, 2H, -NCH$_2$CH_2-), 1.94 – 1.86 (m, 2H, -NCH$_2$CH_2-), 1.75 – 1-72 (m, 2H, -CH_2-), 1.68 (s, 3H, -C(CH_3)), 1.64 (s, 3H, -C(CH_3)), 1.53 – 1.47 (m, 2H, -CH_2-), 1.40 – 1.30 (m‘, 8H, 4 × -CH_2-), 1.26 (s, 3H, -C*(CH$_3$)), 0.92 – 0.86 (m‘, 6H, 2 × -CH$_2$CH_3).

^{13}C-NMR (151 MHz, CD_2Cl_2, 295 K)

δ [ppm]: 170.9 (4 × quart.), 142.9 (4 × quart.), 142.7 (3 × quart.), 128.5 (2 × tert.), 128.2 (tert.), 128.1 (tert.), 126.8 (tert.), 124.2 (tert.), 123.8 (tert.), 123.6 (tert.), 122.5 (tert.), 110.1 (2 × tert.), 87.2 (2 × tert.), 49.7 (2 × quart.), 44.1 (2 × sec.), 32.0 (sec.), 31.9 (sec.), 30.1 (prim.), 27.4 (sec.), 27.2 (sec.), 27.0 (sec.), 26.9 (prim.), 26.9 (prim.), 26.0 (sec.), 23.0 (sec.), 22.9 (sec.), 14.2 (prim.), 14.1 (prim.).

ESI-MS (pos., high res.): $[C_{43}H_{50}N_2O_2]^{\cdot+}$

calcd.: 626.38668

exp.: 626.38773 Δ = 1.68 ppm

Synthesis of compound 8

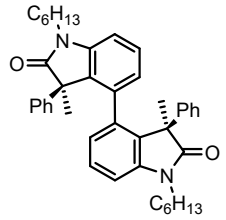

Following a synthetic protocol reported in the literature,[9] Ni(COD)$_2$ (59.8 mg, 217 µmol), COD (30.0 µl, 245 µmol) and 2,2-bipyridine (34.0 mg, 218 µmol) were dissolved in degassed THF (1.5 ml) under a nitrogen atmosphere and stirred at 60 °C for 30 min. Compound **7** (60.0 mg, 155 µmol) in degassed THF (4.5 ml) was added dropwise. After stirring at 70 °C for 16 h and at 80 °C for 2 h the solvent was removed in vacuo. The crude product was purified by flash column chromatography (SiO_2, eluent: DCM → DCM/MeOH 99:1).

Yield: 20.0 mg (32.6 µmol, 42 %) of a colourless solid.

$C_{42}H_{48}N_2O_2$ [612.84]

^{1}H-NMR (400 MHz, $CDCl_3$, 295 K)

δ [ppm]: 7.26 – 7.23 (m', 6H, Ph*H*), 6.93 – 6.91 (m, 4H, Ph*H*), 6.82 (dd, 2H, ^{3}J = 7.9 Hz, ^{4}J = 1.1 Hz, -C*H*-), 6.74 (dd, 2H, ^{3}J = 7.9 Hz, ^{3}J = 7.8 Hz), 5.54 (dd, 2H, ^{3}J = 7.8 Hz, ^{4}J = 1.1 Hz, -CH-), 3.88 – 3.81 (m, 2H, -NCH_2-), 3.63 – 3.56 (m, 2H, -NCH_2-), 1.74 – 1.67 (m, 4H, -NCH$_2$CH_2-), 1.35 (s, 6H, 2 × -C(Ph)CH_3), 1.32 – 1.25 (m, 12H, 6 × -CH_2-), 0.86 (t, 6H, ^{3}J = 7.1 Hz, 2 × -CH$_2$CH_3).

^{13}C-NMR (101 MHz, $CDCl_3$, 295 K)

δ [ppm]: 179.5 (quart.), 143.4 (quart.), 142.6 (quart.), 135.6 (quart.), 133.1 (quart.), 128.7 (tert.), 127.2 (tert.), 127.1 (tert.), 126.4 (tert.), 124.9 (tert.), 107.8 (tert.), 52.4 (quart.), 40.2 (sec.), 31.6 (sec.), 27.4 (sec.), 26.6 (sec.), 22.6 (sec.), 18.7 (prim.), 14.1 (prim.).

ESI-MS (pos.): $[C_{42}H_{48}N_2O_2 + Na]^+$

calcd.: 635.3608

exp.: 635.3603

Synthesis of (*P*)-dSQA

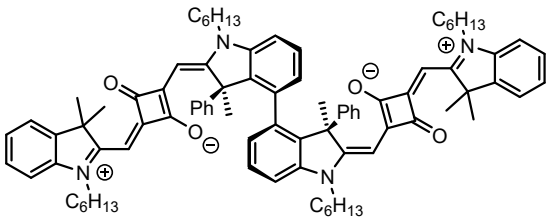

Following a synthetic protocol reported in the literature,[10] compound **8** (32.0 mg, 52.2 µmol) was dissolved in THF (1 ml) under a nitrogen atmosphere and a solution of MeMgBr in Et_2O (0.130 ml, 3 M, 390 µmol) was added. After stirring at 60 °C for 2 h, MeOH (0.2 ml) was added and the solvent was removed in vacuo. The residue was treated with an aqueous HCl solution (2 M, 0.5 ml) and extracted with DCM (3 × 10 ml). The combined organic phases were dried over $MgSO_4$ and the solvent was removed in vacuo. Due to the instability of the compound, the crude product **9** was used without further purification.

Compounds **9** (35.0 mg, 51.3 µmol) and **10** (34.8 mg, 103 µmol) were dissolved in a 1:1 mixture of toluene and 1-butanol (20 ml) and NEt_3 (1 ml). Using a Dean-Stark-trap, the mixture was heated at 135 °C for 18 h. The solvent was removed in vacuo. The crude product was purified by flash column chromatography (SiO_2, eluent: DCM/MeOH 99.5:0.5 → 98:2) and GPC (eluent: DCM).

Yield: 31.0 mg (24.8 µmol, 48 %) of a blue solid.

$C_{86}H_{98}N_4O_4$ [1251.73]

^{1}H-NMR (600 MHz, 1,1,2,2-tetrachloroethane-d_2, 373 K)

δ [ppm]: 7.33 (d, ^3J = 7.4 Hz, 2H, -C*H*-), 7.32 – 7.29 (m, 2H, -C*H*-), 7.26 – 7.22 (m‘, 6H, Ph*H*), 7.16 – 7.13 (m, 2H, -C*H*-), 7.03 (d, ^3J = 8.0 Hz, 2H, -C*H*-), 6.99 – 6.96 (m’, 6H, 4 × Ph*H*, 2 × -C*H*-), 6.84 – 6.81 (m, 2H, -C*H*-), 5.88 (s, 2H, -CC*H*C-), 5.48 (s, 2H, -CC*H*C-), 5.40 (d, ^3J = 7.4 Hz, 2H, -C*H*-), 4.82 – 4.74 (m, 2H, -NCH_2-), 4.45 – 4.38 (m, 2H, -NCH_2-), 4.01 (t, ^3J = 7.4 Hz, 4H, 2 × -NCH_2-), 1.92 – 1.87 (m, 4H, 2 × -NCH$_2$CH_2-), 1.83 – 1.79 (m, 4H, 2 × -NCH$_2$CH_2-), 1.77 (s, 6H, 2 × -C(CH_3)Ph), 1.73 (s, 6H, 2 × -C(CH_3)$_2$), 1,72 (s, 6H, -C(CH_3)$_2$), 1.55 – 1.51 (m‘, 4H, 2 × -CH_2-), 1.47 – 1.33 (m‘, 20 H, 10 × -CH_2-), 0.95 (t, ^3J = 7.1 Hz, 6H, 2 × -CH$_2$CH_3), 0.92 (t, ^3J = 7.1 Hz, 6H, 2 × -CH$_2$CH_3).

^{13}C-NMR (151 MHz, 1,1,2,2-tetrachloroethane-d_2, 373 K)

δ [ppm]: 181.6 (quart.), 180.1 (quart.), 178.9 (quart.), 170.2 (quart.), 169.1 (quart.), 144.3 (quart.), 143.2 (quart.), 142.4 (quart.), 142.1 (quart.), 137.0 (quart.), 134.7 (quart.), 128.3 (tert.), 127.5 (tert.), 127.2 (tert.), 127.0 (tert.), 126.9 (tert.), 126.4 (tert.), 123.6 (tert.), 122.0 (tert.), 109.3 (2 ×tert.), 87.0 (2 × tert.), 57.2 (quart.), 49.1 (quart.), 44.5 (sec.), 43.6 (sec.), 31.3 (sec.), 31.2 (sec.), 26.9 (2 × prim.), 26.8 (2 × sec.), 26.5 (sec.), 26.4 (sec.), 22.2 (sec.), 22.1 (sec.), 21.8 (prim.), 13.6 (prim.), 13.5 (prim.).

ESI-HRMS (pos.): $[C_{86}H_{98}N_4O_4]^{\cdot+}$

theoret.: 1250.75826

exp.: 1250.75732 *Δ* = 0.75 ppm

Synthesis of (*P*)-dSQB

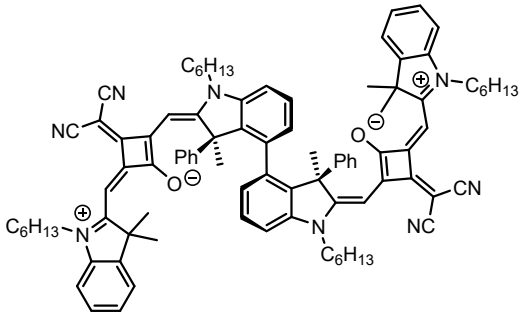

Following a synthetic protocol reported in the literature,[10] compound **8** (23.0 mg, 37.5 µmol) was dissolved in THF (1 ml) under a nitrogen atmosphere and a solution of MeMgBr in Et_2O (0.100 ml, 3 M, 300 µmol) was added. After stirring at 60 °C for 2 h, MeOH (0.2 ml) was added and the solvent was removed in vacuo. The residue was treated with an aqueous HCl solution (2 M, 0.5 ml) and extracted with DCM (3 × 10 ml). The combined organic phases were dried over $MgSO_4$ and the solvent was removed in vacuo. Due to the instability of the compound, the crude product **9** was used without further purification.

Compounds **9** (25.0 mg, 36.7 µmol) and **11** (39.3 mg, 80.4 µmol) were dissolved in a 1:1 mixture of toluene and 1-butanol (20 ml) and NEt_3 (1 ml). Using a Dean-Stark-trap, the mixture was stirred at 135 °C for 4 h. The solvent was removed *in vacuo*. The crude product was purified by flash column chromatography (SiO_2, eluent: DCM/MeOH 99.75:0.25 → 99:1) and GPC (eluent: DCM).

Yield: 21.0 mg (15.6 µmol, 42 %) of a blue solid.

$C_{92}H_{98}N_8O_2$ [1347.82]

^{1}H-NMR (600 MHz, CD_2Cl_2, 295 K)

δ [ppm]: 7.36 (d, ^3J = 7.4 Hz, 2H, Ph*H*), 7.35 – 7.32 (m, 2H, Ph*H*), 7.22 – 7.19 (m‘, 4H, Ph*H*), 7.17 – 7.14 (m‘, 4H, -C*H*- ach. Ind.), 7.08 (d, ^3J = 8.1 Hz, 2H, Ph*H*), 7.06 (d, ^3J =7.9 Hz, 2H, ch. Ind.), 7.01 – 6.90 (m‘, 4H, -C*H*- ach. Ind.), 6.83 – 6.80 (m, 2H, -C*H*- ch. Ind.), 6.35 (s, 2H, -CC*H*C-), 6.10 (s, 2H, -CC*H*C-), 5.27 (d, ^3J = 7.4 Hz, 2H, -C*H*- ch. Ind.), 4.37 – 4.23 (m, 4H, -NCH_2-), 3.97 – 3.91 (m, 4H, -NCH_2-), 1.96 (m‘, 8H, -CH_2-), 1.73 (m, 4H, -NCH$_2$CH_2-), 1.67 (s, 6H, -C(CH_3)Ph), 1.56 (s, 6H, -C(CH_3)$_2$), 1.54 (s, 6H, -C(CH_3)$_2$), 1.43 – 1.35 (m‘, 12 H, -CH_2-), 1.32 – 1.26 (m‘, 8 H, -CH_2-), 0.92 (t, ^3J =7.1 Hz, 6H, -CH$_2$CH_3), 0.86 (t, ^3J =7.1 Hz, 6H, -CH$_2$CH_3).

^{13}C-NMR (151 MHz, CD_2Cl_2, 295 K)

δ [ppm]: 173.3 (quart.), 172.5 (quart.), 171.4 (quart.), 167.5 (quart.), 167.1 (quart.), 166.0 (quart.), 143.8 (quart.), 142.9 (quart.), 142.7 (quart.), 142.3 (quart.), 138.4 (quart.), 134.8 (quart.), 128.5 (tert.), 128.3 (tert.), 128.0 (tert.), 127.9 (tert.), 127.7 (1 × tert.), 125.0 (tert.), 122.5 (tert.), 119.2 (quart.), 119.1 (quart.), 110.7 (tert.), 110.5 (tert.), 89.5 (tert.), 88.9 (tert.), 57.7 (quart.), 49.8 (quart.), 45.4 (sec.), 44.9 (sec.), 40.2 (quart.), 31.9 (sec.), 31.8 (sec.), 27.6 (sec.), 27.5 (sec.), 26.9 (prim.), 26.7 (1 × sec., 1 × prim.), 26.1 (prim.), 23.0 (sec.), 22.8 (sec.), 21.5 (sec.),14.2 (prim.), 14.1 (prim.).

ESI-HRMS (pos.): $[C_{92}H_{98}N_8O_2]^{\cdot+}$

calcd.: 1347.78393

exp.: 1347.78418 Δ = 0.19 ppm

Synthesis of (*R*)-mSQB

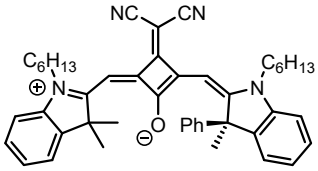

Following a synthetic protocol reported in the literature,[10] compound **16** (20.0 mg, 65.1 µmol) was dissolved in THF (1 ml) under a nitrogen atmosphere and a solution of MeMgBr in Et_2O (0.100 ml, 3 M, 300 µmol) was added. After stirring at 60 °C for 2 h, MeOH (0.2 ml) was added and the solvent was removed in vacuo. The residue was treated with an aqueous HCl solution (2 M, 0.5 ml) and extracted with DCM (3 × 10 ml). The combined organic phases were dried over $MgSO_4$ and the solvent was removed *in vacuo*. Due to the instability of the compound, the crude product **17** was used without further purification.

Compounds **17** (22.2 mg, 64.9 µmol) and **11** (38.0 mg, 77.8 µmol) were dissolved in a 1:1 mixture of toluene and 1-butanol (20 ml) and NEt_3 (1 ml). Using a Dean-Stark-trap, the mixture was stirred at 135 °C for 4 h. The solvent was removed *in vacuo*. The crude product was purified by flash column chromatography (SiO_2, eluent: DCM → DCM/MeOH 99.5:0.5) and GPC (eluent: DCM).

Yield: 22.0 mg (32.6 µmol, 50 %) of a green solid.

$C_{46}H_{50}N_4O$ [674.92]

^{1}H-NMR (600 MHz, CD_2Cl_2, 295 K)

δ [ppm]: 7.51 (d, ^3J = 7.3 Hz, 1H, -C*H*-), 7.40 – 7.34 (m', 6H, -C*H*-), 7.28 – 7.21 (m', 4H, -C*H*-), 7.13 (m', 2H, -C*H*-), 6.58 (s, 1H, -CC*H*C-), 6.40 (s, 1H, -CC*H*C-), 4.31 – 4.20 (m, 2H, -NCH_2-), 4.09 – 4.06 (m, 2H, -NCH_2-), 2.27 (s, 3H, -C(CH_3)Ph), 1.96 – 1.93 (m, 2H, -NCH$_2$CH_2-), 1.79 – 1.74 (m, 2H, -NCH$_2$CH_2-), 1.66 (s, 3H, -C(CH_3)$_2$), 1.61 – 1.55 (m, 2H, -CH_2-), 1.49 – 1.39 (m', 4H, -CH_2-), 1.38 – 1.28 (m', 9H, 1 × -C(CH_3)$_2$, 3 × -CH_2-), 0.91 (t, ^3J = 7.3 Hz, 3H, -CH$_2$CH_3), 0.86 (t, ^3J = 7.1 Hz, 3H, -CH$_2$CH_3).

^{13}C-NMR (151 MHz, CD_2Cl_2, 295 K)

δ [ppm]: 173.5 (quart.), 172.4 (quart.), 170.8 (quart.), 168.1 (quart.), 166.9 (quart.) 166.7 (quart.), 143.4 (quart.), 143.3 (quart.), 143.0 (quart.), 142.9 (quart.), 142.8

(quart.), 142.7 (quart.), 129.1 (tert.), 129.0 (tert.), 129.0 (tert.), 127.4 (tert.), 127.3 (tert.), 125.8 (tert.), 125.3 (tert.), 124.2 (tert.), 123.1 (tert.), 119.4 (quart.), 119.4 (quart.), 111.9 (tert.), 111.5 (tert.), 89.8 (tert.), 89.7 (tert.), 57.8 (quart.), 50.3 (quart.), 45.2 (sec.), 45.1 (sec.), 32.3 (sec.), 32.2 (sec.), 28.0 (sec.), 28.0 (sec.), 27.1 (sec.), 26.9 (sec.), 26.8 (prim.), 26.2 (prim.), 25.8 (prim.), 23.2 (sec.), 23.1 (sec.), 14.3 (prim.), 14.2 (prim.).

ESI-HRMS (pos.): $[C_{46}H_{50}N_4O]^{\cdot+}$

calcd.: 674.39791

exp.: 674.39974 Δ = 2.71 ppm

Synthesis of compound 13

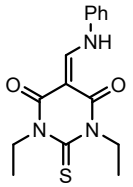

Following a synthetic protocol reported in the literature,[11] compound **12** (100 mg, 499 µmol), aniline (50.0 µl, 51.1 mg, 549 µmol) and diethoxymethoxyethane (130 µl, 116 mg, 783 µmol) were dissolved in MTBE (1 ml) and stirred at 60 °C for 3 h under a nitrogen atmosphere. The yellow solution was washed with water and dried over Na_2SO_4. The solvent was removed in vacuo and the crude product was purified by column chromatography (SiO_2, eluent: DCM).

Yield: 141 mg (465 µmol, 93 %) of a yellow solid.

^{1}H-NMR (600 MHz, CD_2Cl_2, 295 K)

$C_{15}H_{17}N_3O_2S$ [303.38]

δ [ppm]: 12.33 (d, ^3J = 13.8 Hz, 1H, -N*H*Ph), 8.74 (d, ^3J = 13.8 Hz, 1H, -C*H*NH-), 7.47 – 7.43 (m, 2H, Ph*H*), 7.31 – 7.26 (m', 3H, Ph*H*), 4.59 – 4.54 (m', 4H, -NCH_2-), 1.34 – 1.18 (m', 6H, -NCH$_2H_3$).

^{13}C-NMR (151 MHz, CD_2Cl_2, 295 K)

δ [ppm]: 179.0 (quart.), 163.3 (quart.), 161.0 (quart.), 153.0 (tert.), 138.0 (quart.), 130.3 (2 × tert.), 127.2 (tert.), 118.3 (tert.), 95.0 (quart.), 43.2 (sec.), 42.6 (sec.), 12.6 (prim.), 12.4 (prim.).

MALDI-MS (pos.): $[C_{15}H_{17}N_3O_2S + H]^{\cdot+}$

calcd.: 304.1114

exp.: 304.10337

Synthesis of (*R*)-mMC

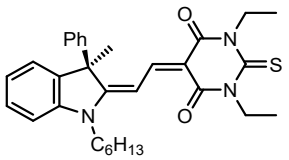

Following a synthetic protocol reported in literature,[12] compounds **17** (33.0 mg, 96.5 µmol) and **13** (23.0 mg, 75.8 µmol) were dissolved in ethanol (1 ml) under a nitrogen atmosphere. After stirring at 80 °C for 5 min, piperidine (10.0 µl, 8.62 mg, 101 µmol) was added and the mixture was stirred at 80 °C for 19 h. The solvent was removed in vacuo and the crude product was purified by column chromatography (SiO_2, eluent: DCM → DCM/MeOH 99:1) and GPC (eluent: DCM).

Yield: 34.0 mg (65.9 µmol, 87 %) of a red solid.

$C_{31}H_{37}N_3O_2S$ [515.71]

^{1}H NMR (600 MHz, $CDCl_3$, 295 K)

δ [ppm]: 8.14 (d, ^3J = 14.2 Hz, 1H, -C*H*-), 7.72 (d, ^3J = 14.2 Hz, 1H, -C*H*-), 7.37 – 7.33 (m', 3H, 1 × -C*H*-, 2 × Ph*H*), 7.28 – 7.27 (m, 1H, Ph*H*), 7.22 – 7.21 (m', 2H, Ph*H*), 7.12 – 7.10 (m', 2H, -C*H*-), 7.05 – 7.04 (m, 1H, -C*H*-), 4.53 (q, ^3J = 6.9 Hz, 2H, -NCH_2CH$_3$), 4.47 (q, ^3J = 7.0 Hz, 2H, -NCH_2CH$_3$), 4.16 – 4.07 (m, 2H, -NCH_2CH$_2$-), 2.02 (s, 3H, -C(CH_3)Ph), 1.97 – 1.92 (m, 2H, -NCH$_2$CH_2-), 1.54 – 1.49 (m, 2H, -CH_2-), 1.43 – 1.38 (m, 2H, -CH_2-), 1.38 – 1.33 (m, 2H, -CH_2-), 1.28 (t, ^3J = 7.0 Hz, 3H, -NCH$_2$CH_3), 1.22 (t, ^3J = 6.9 Hz, 3H, -NCH$_2$CH_3), 0.91 (t, ^3J = 7.2 Hz, 3H, -CH$_2$CH_3).

^{13}C NMR (151 MHz, $CDCl_3$, 295 K)

δ [ppm]: 178.7 (quart.), 177.2 (quart.), 161.5 (quart.), 161.2 (quart.), 154.4 (tert.), 142.3 (quart.), 142.1 (quart.), 141.9 (quart.), 129.4 (tert.), 128.6 (tert.), 128.0 (tert.), 125.9 (tert.), 125.2 (tert.), 123.7 (tert.), 110.4 (tert.), 103.8 (quart.), 99.0 (tert.), 56.3 (quart.), 44.5 (sek.), 43.3 (sec.), 42.7 (sec.), 31.6 (sec.), 27.7 (prim.), 27.3 (sec.), 26.9 (sec.), 22.6 (sec.), 14.1 (prim.), 12.7 (prim.), 12.6 (prim.).

ESI-HRMS (pos.): $[C_{31}H_{37}N_3O_2S + Na]^+$

calcd.: 538.24987

exp.: 538.25129 *Δ* = 2.64 ppm

Synthesis of (*P*)-dMC

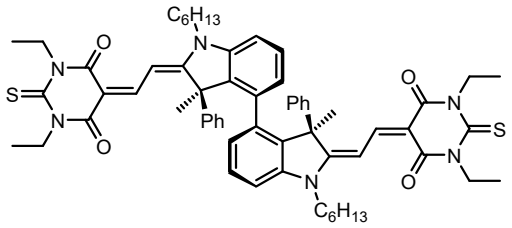

Following a synthetic protocol reported in literature,[12] compounds **9** (20.0 mg, 29.3 µmol) and **13** (17.8 mg, 58.7 µmol) were dissolved in ethanol (1 ml). After stirring at 80 °C for 5 min, piperidine (5 µl, 4 mg, 0.05 mmol) was added and the mixture was stirred for at 80 °C 17 h. The solvent was removed in vacuo and the crude product was purified by column chromatography (SiO_2, eluent: DCM/MeOH 99.5:0.5) and GPC (eluent: DCM).

Yield: 16.0 mg (15.5 µmol, 53 %) of a red solid.

$C_{62}H_{72}N_6O_4S_2$ [1029.41]

^{1}H-NMR (600 MHz, THF-d_8, 295 K)

δ [ppm]: 8.20 (d, ^3J = 14.2 Hz, 2H, -C*H*-), 7.65 (d, ^3J = 14.2 Hz, 2H, -C*H*-), 7.32 (d, ^3J = 7.6 Hz, 2H, -C*H*-), 7.29 – 7.23 (m', 6H, Ph*H*), 7.11 – 6.88 (m, 4H, Ph*H*), 6.85 (m, 2H, -C*H*-), 5.26 (d, ^3J = 7.6 Hz, 2H, -C*H*-), 4.46 (q, ^3J = 6.9 Hz, 4H, -NCH_2CH$_3$), 4.42 – 4.35 (m, 4H, - NCH_2CH$_3$), 4.17 (t, ^3J = 5.0 Hz, 4H, -NCH_2-), 1.97 – 1.92 (m, 4H, -NCH$_2$CH_2-), 1.75 (s, 6H, -C(CH_3)Ph), 1.60 – 1.55 (m, 4H, -CH_2-), 1.48 – 1.45 (m, 4H, -CH_2-), 1.41 – 1.35 (m, 4H, -CH_2-), 1.16 (t, ^3J = 6.9 Hz, 6H, -NCH$_2$CH_3), 1.12 (t, ^3J = 6.9 Hz, 6H, -NCH$_2$CH_3), 0.94 (t, ^3J = 7.3 Hz, 6H, -CH$_2$CH_3),

^{13}C-NMR (151 MHz, $CDCl_3$, 295 K)

δ [ppm]: 178.4 (quart.), 175.6 (quart.), 160.5 (quart.), 160.1 (quart.), 152.9 (tert.), 143.7 (quart.), 143.3 (quart.), 137.7 (quart.), 134.2 (quart.), 128.9 (2 × tert.), 127.7 (tert.), 127.4 (tert.), 127.1 (tert.), 103.4 (quart.), 97.7 (tert.), 66.9 (tert.), 56.3 (quart.), 43.8 (sec.), 42.2 (sec.), 41.6 (sec.), 31.4 (sec.), 26.6 (2 × sec.), 24.8 (prim.), 22.5 (sec.), 13.4 (prim.), 11.9 (prim.), 11.7 (prim.).

ESI-HRMS (pos.): $[C_{46}H_{50}NaN_4O]^{\cdot+}$

calcd.: 1053.49837[1]

exp.: 1053.49872[1] Δ = 0.33 ppm

Δ = 0.33 ppm[1] The given value ist he one of third highest intensity.

8 NMR spectra

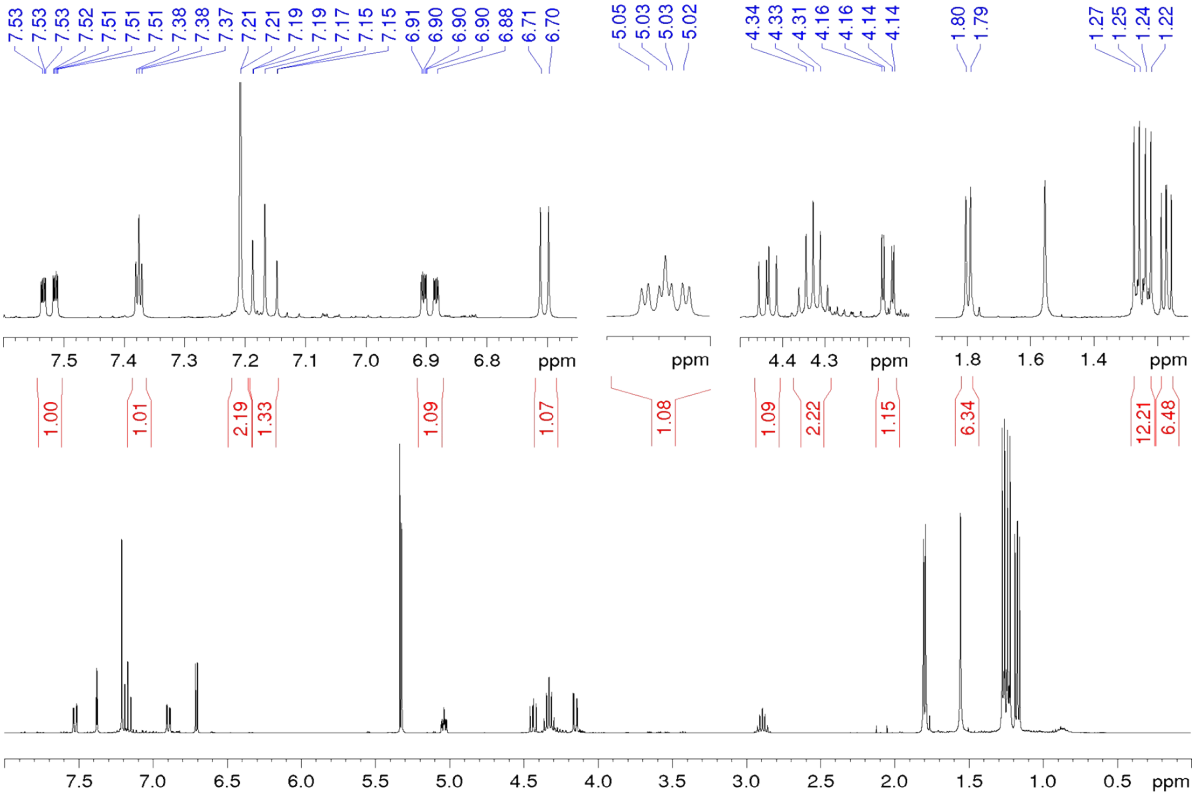

Fig. S27 ^{1}H NMR spectrum of **4**.

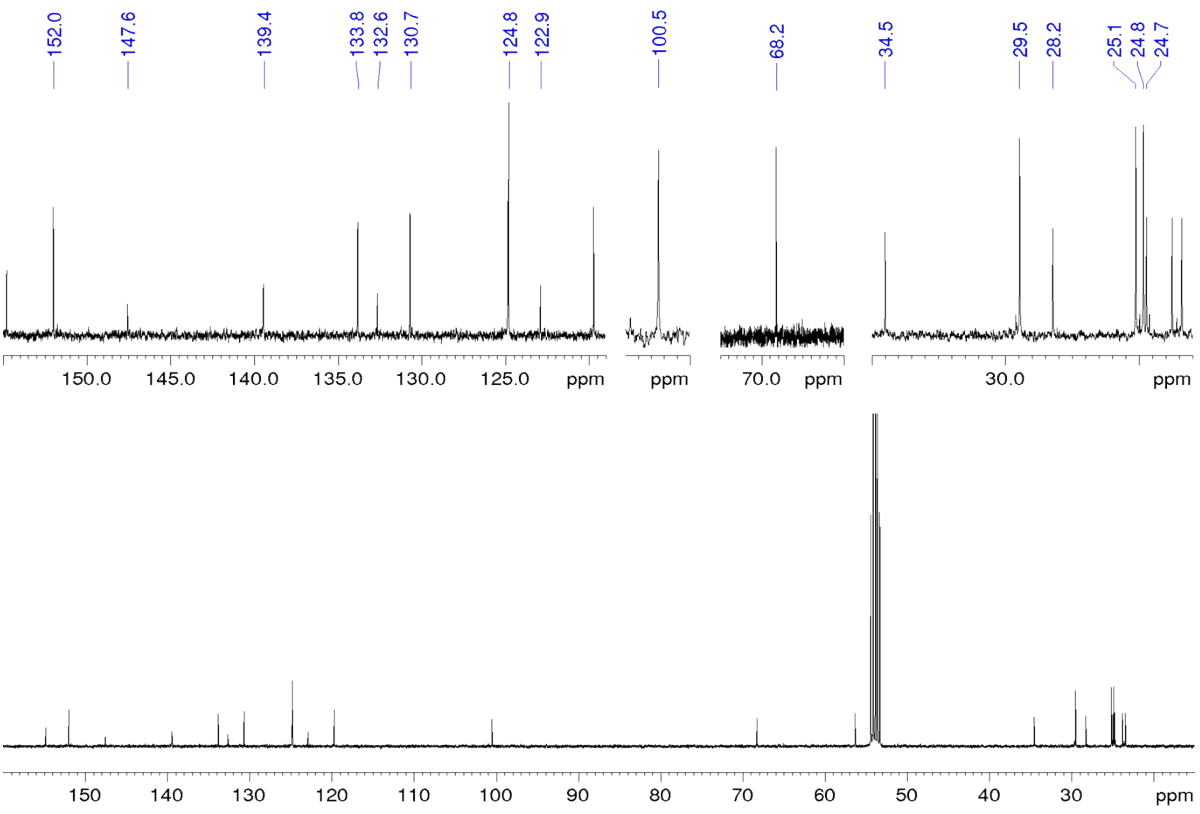

Fig. S28 ^{13}C NMR spectrum of **4**.

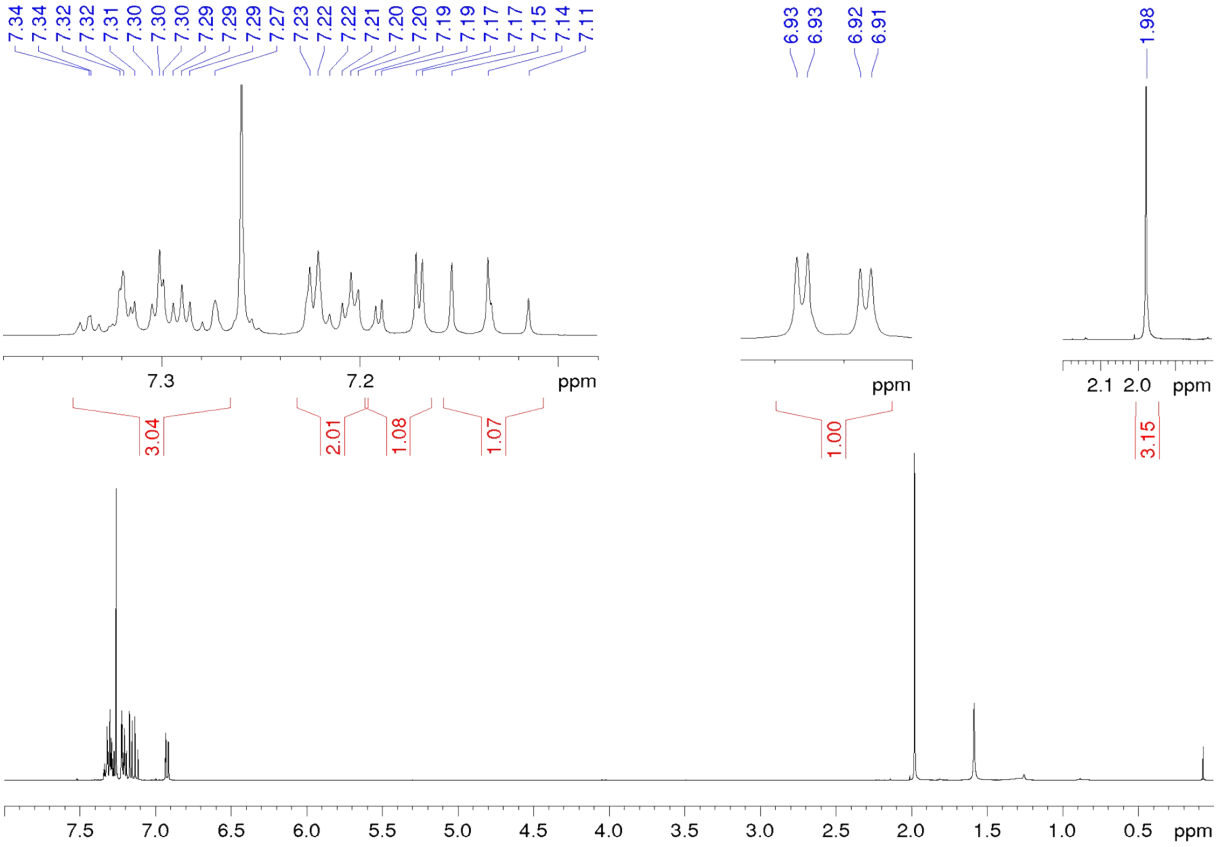

Fig. S29 ^{1}H NMR spectrum of **5**.

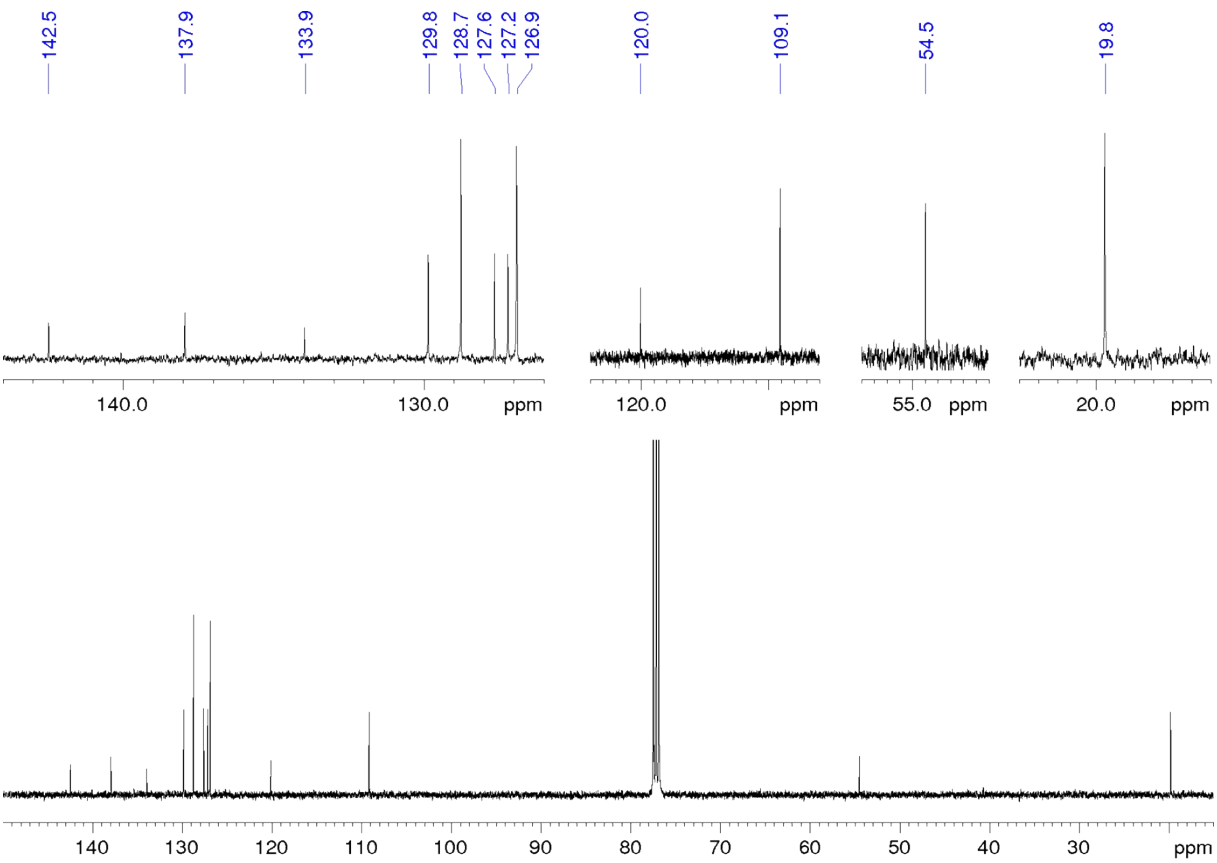

Fig. S30 ^{13}C NMR spectrum of **5**.

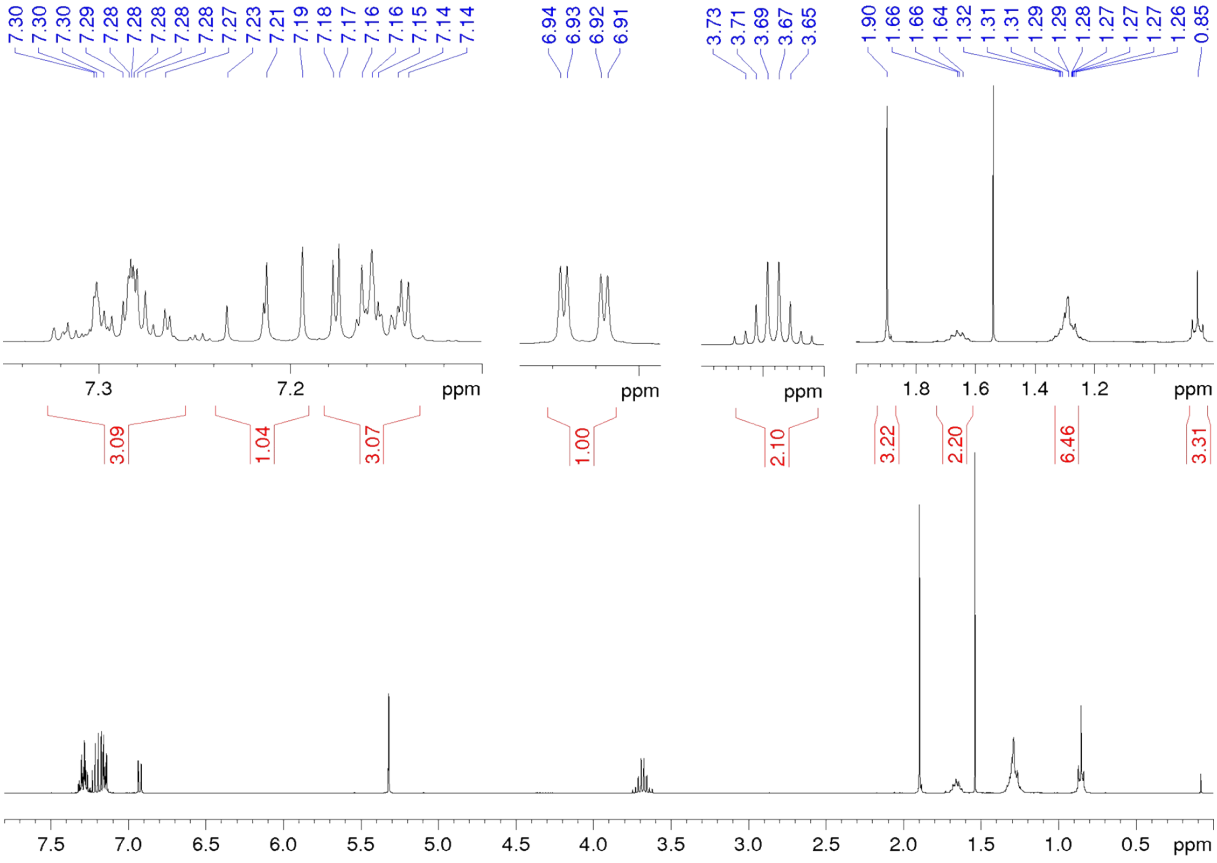

Fig. S31 ^{1}H NMR spectrum of **7**.

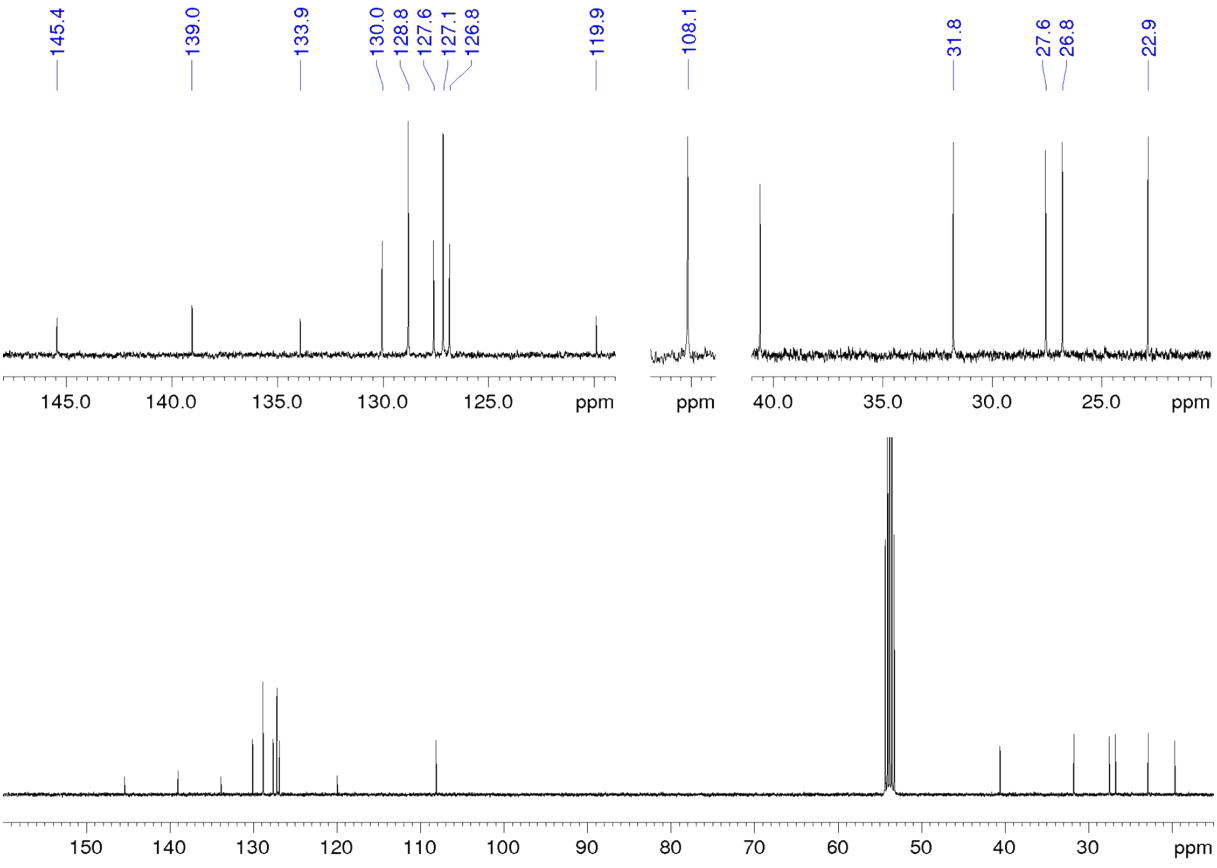

Fig. S32 ^{13}C NMR spectrum of **7**.

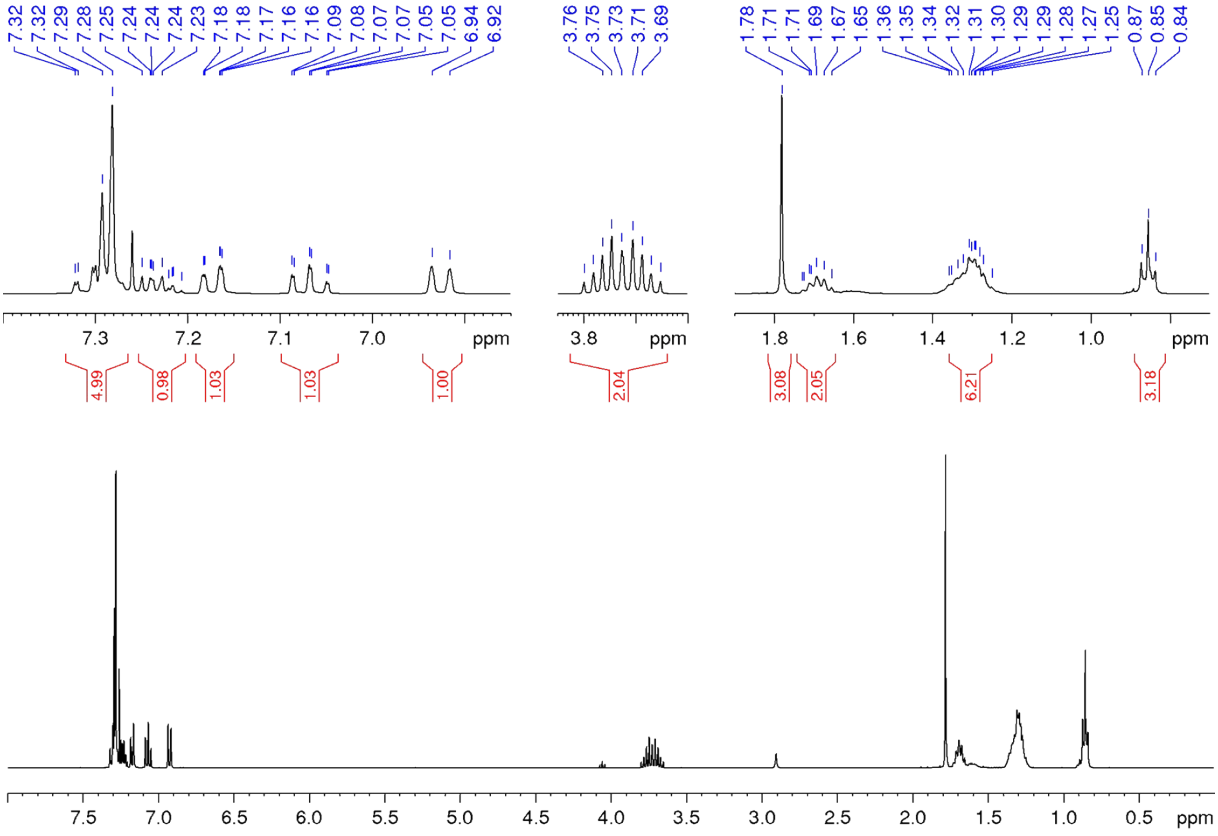

Fig. S33 ^{1}H NMR spectrum of **16**.

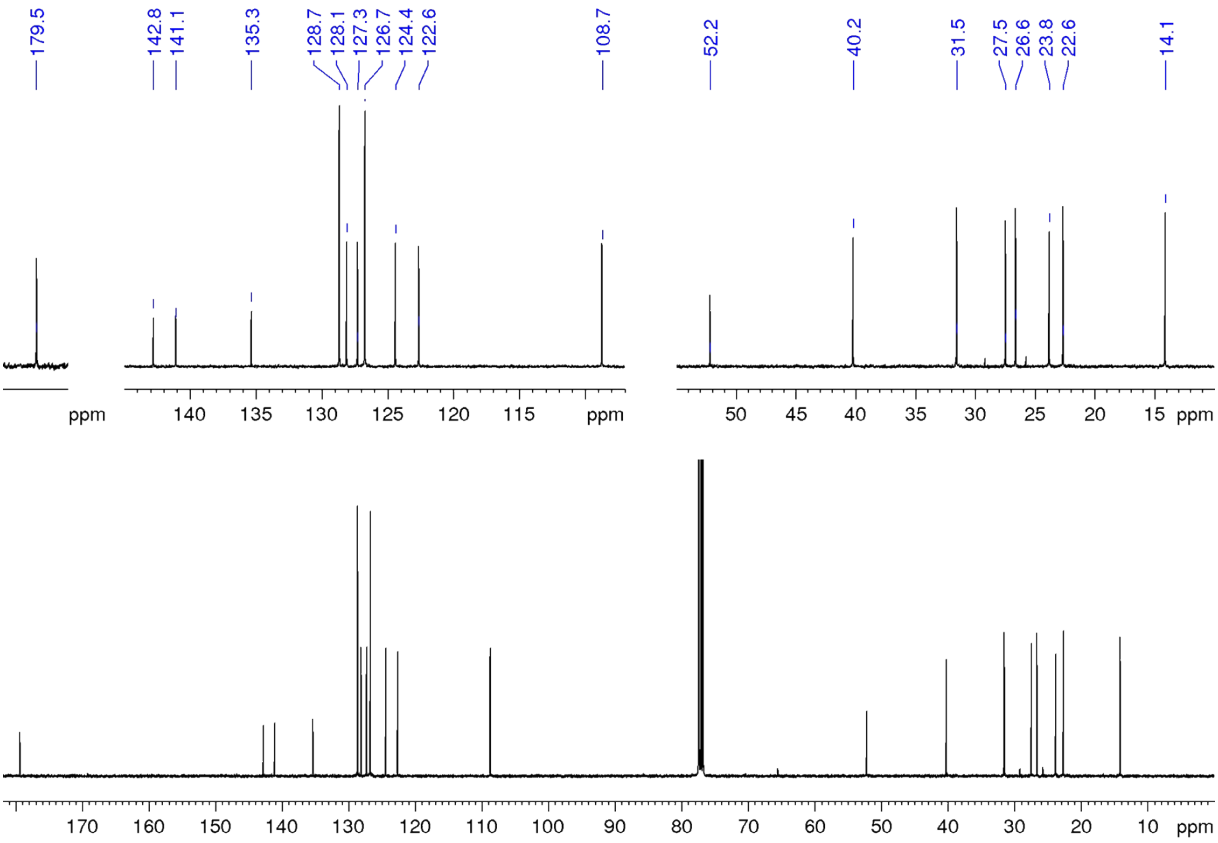

Fig. S34 ^{13}C NMR spectrum of **16**.

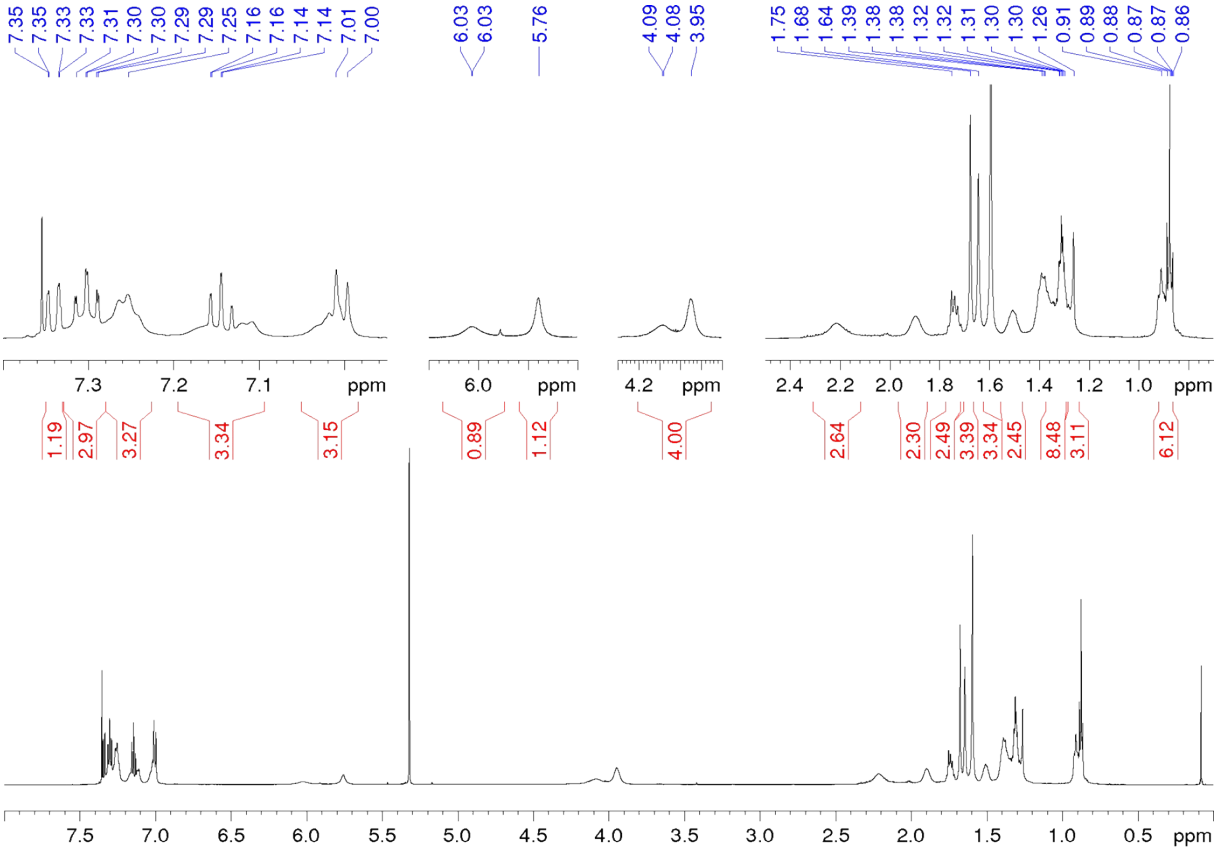

Fig. S35 ^{1}H NMR spectrum of **mSQA**.

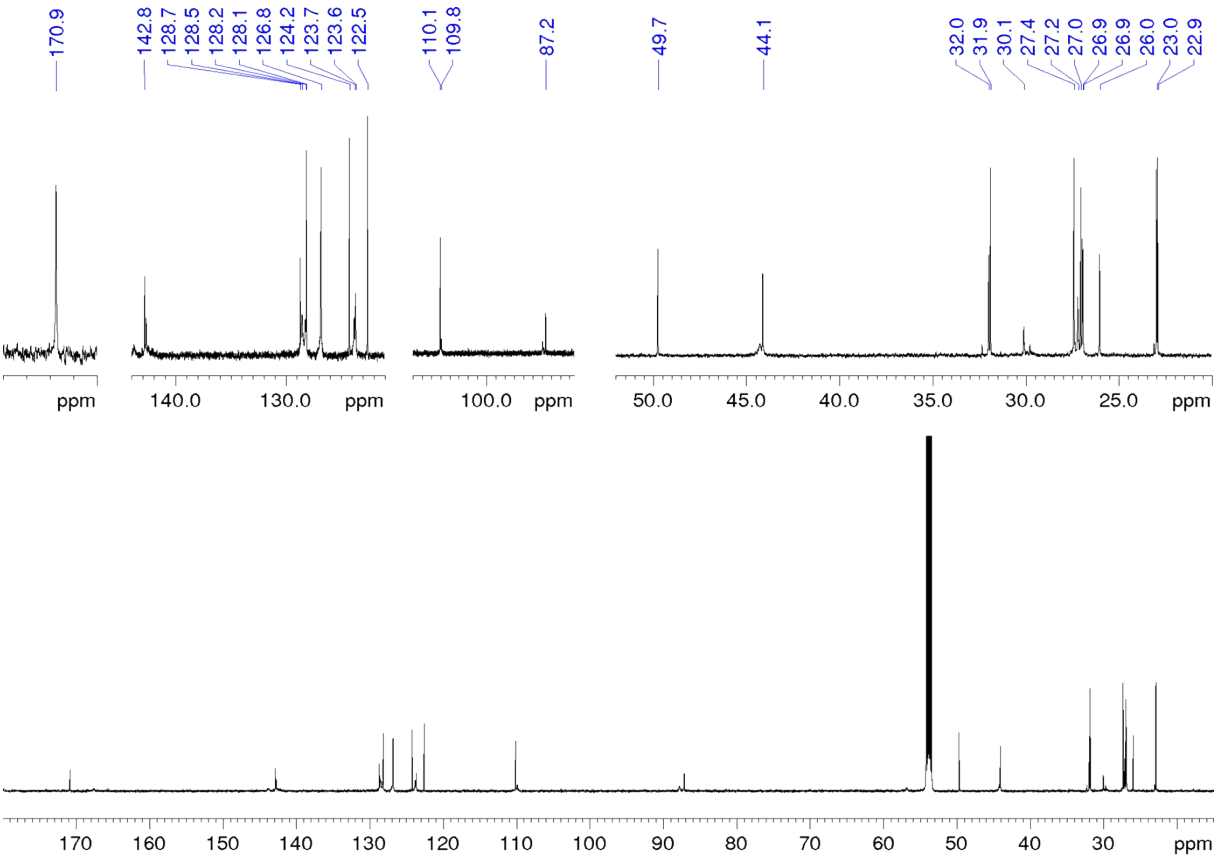

Fig. S36 ^{13}C NMR spectrum of **mSQA**.

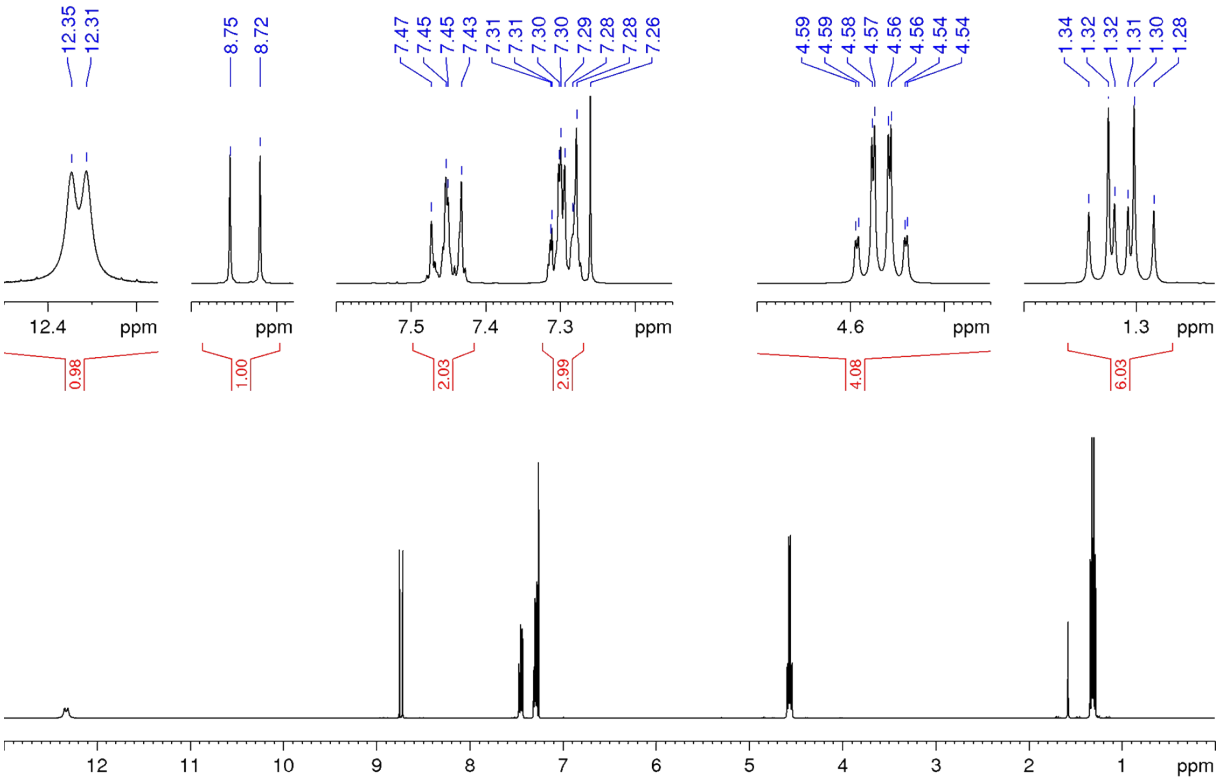

Fig. S37 ^{1}H NMR spectrum of **13**.

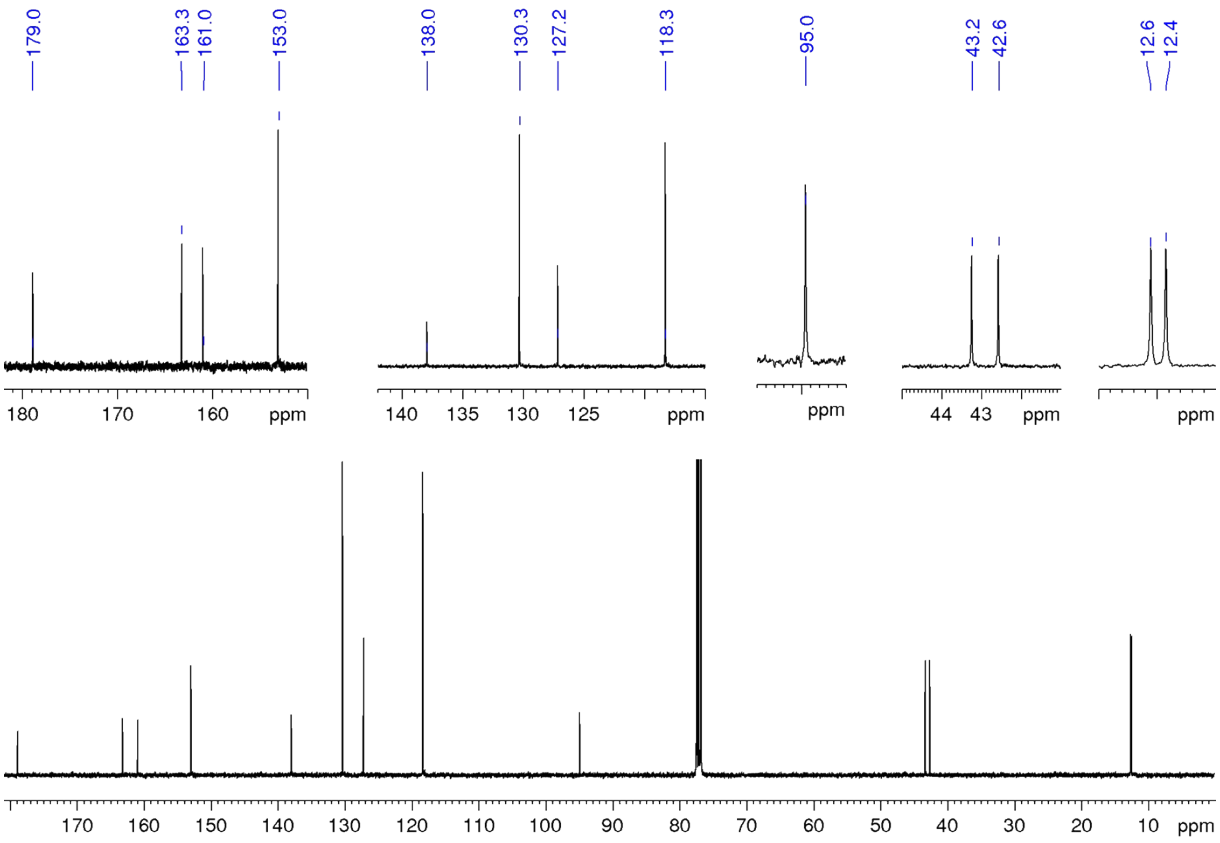

Fig. S38 ^{13}C NMR spectrum of **13**.

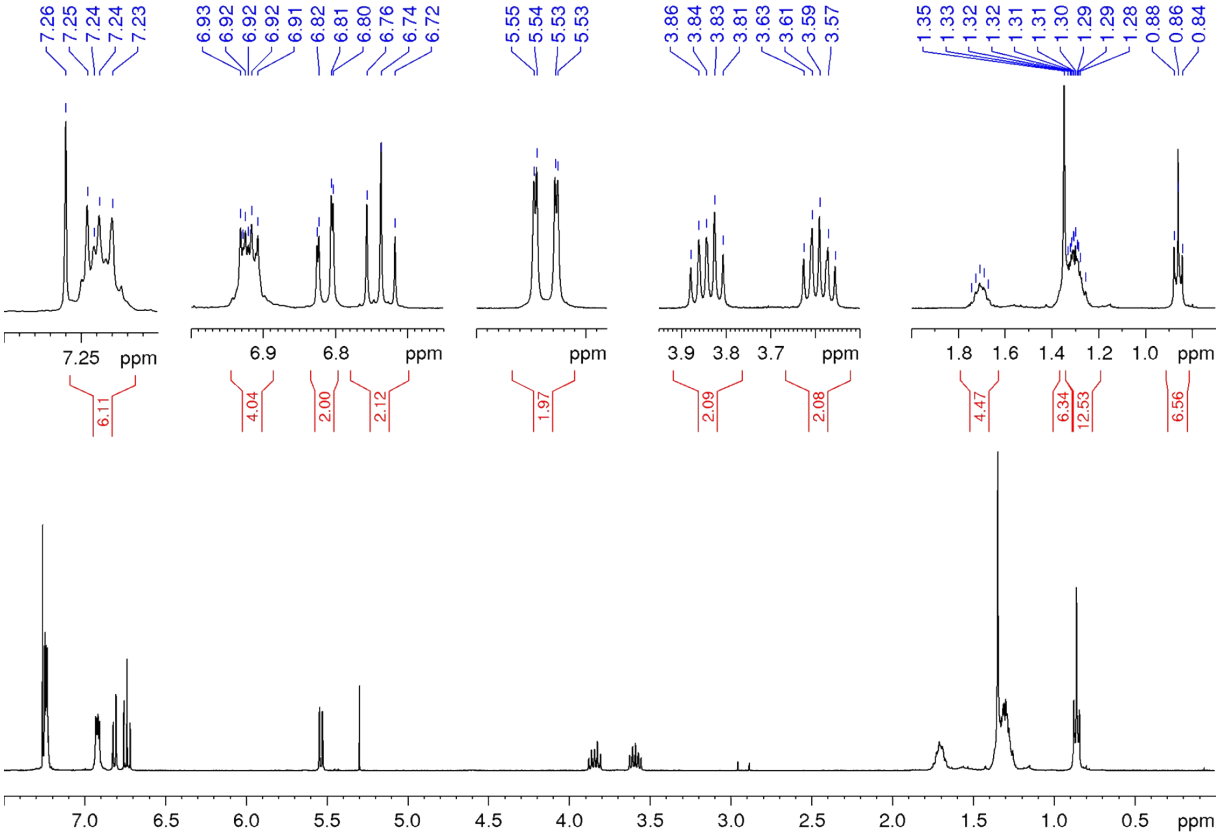

Fig. S39 ^{1}H NMR spectrum of **8**.

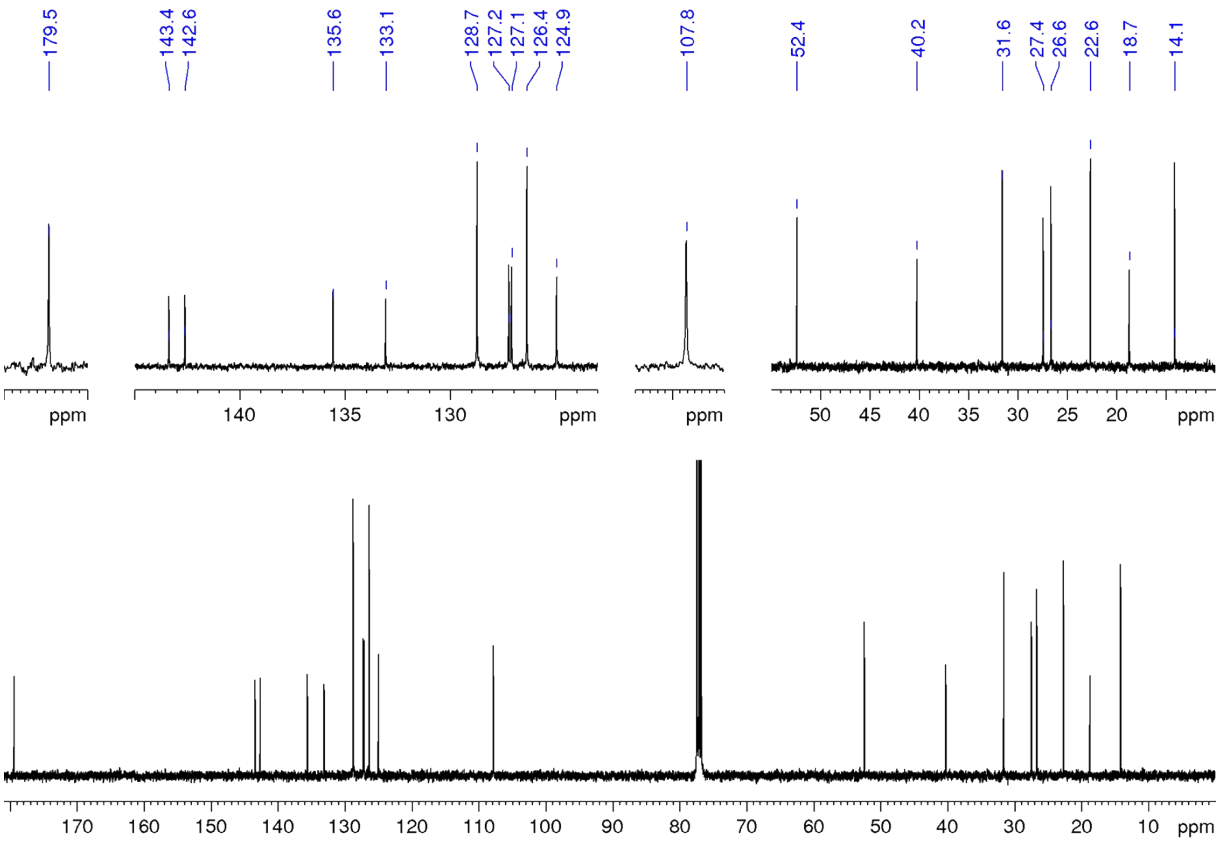

Fig. S40 ^{13}C NMR spectrum of **8**.

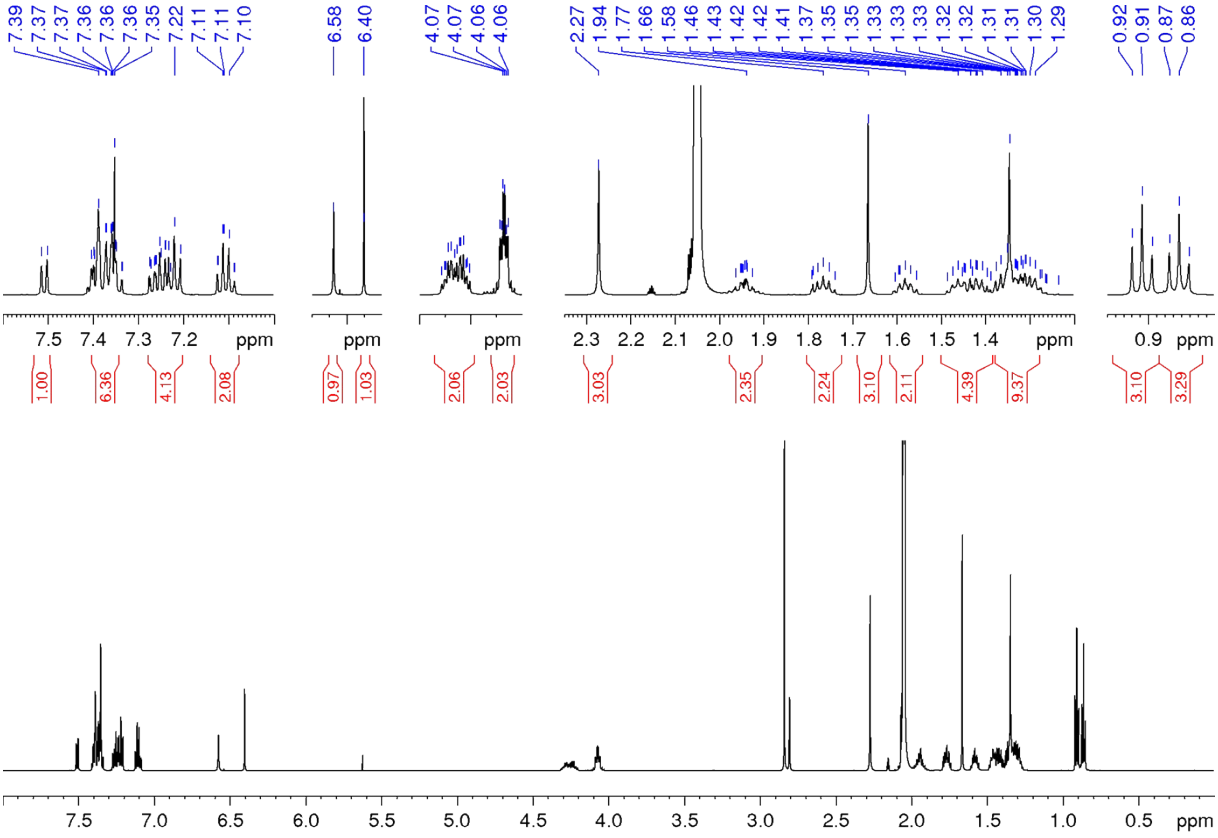

Fig. S41 ^{1}H NMR spectrum of **mSQB**.

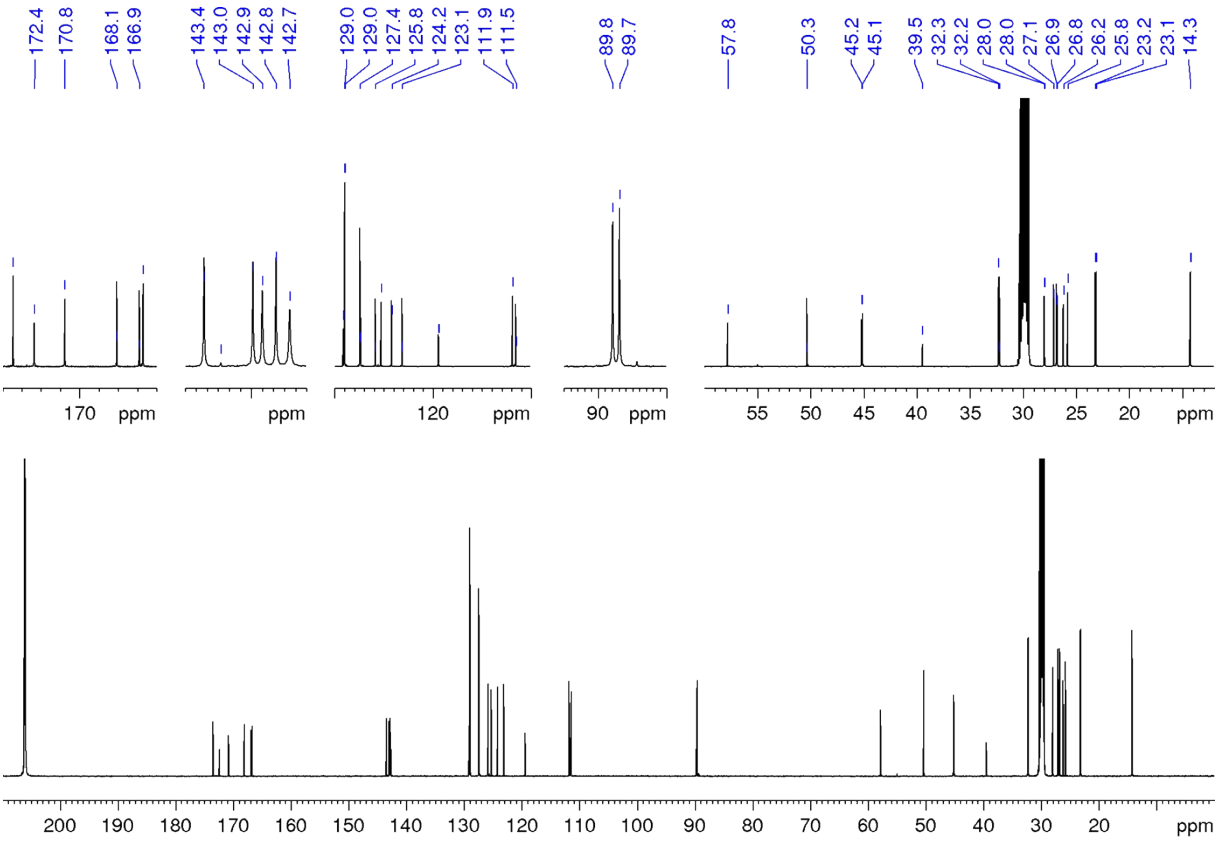

Fig. S42 ^{13}C NMR spectrum of **mSQB**.

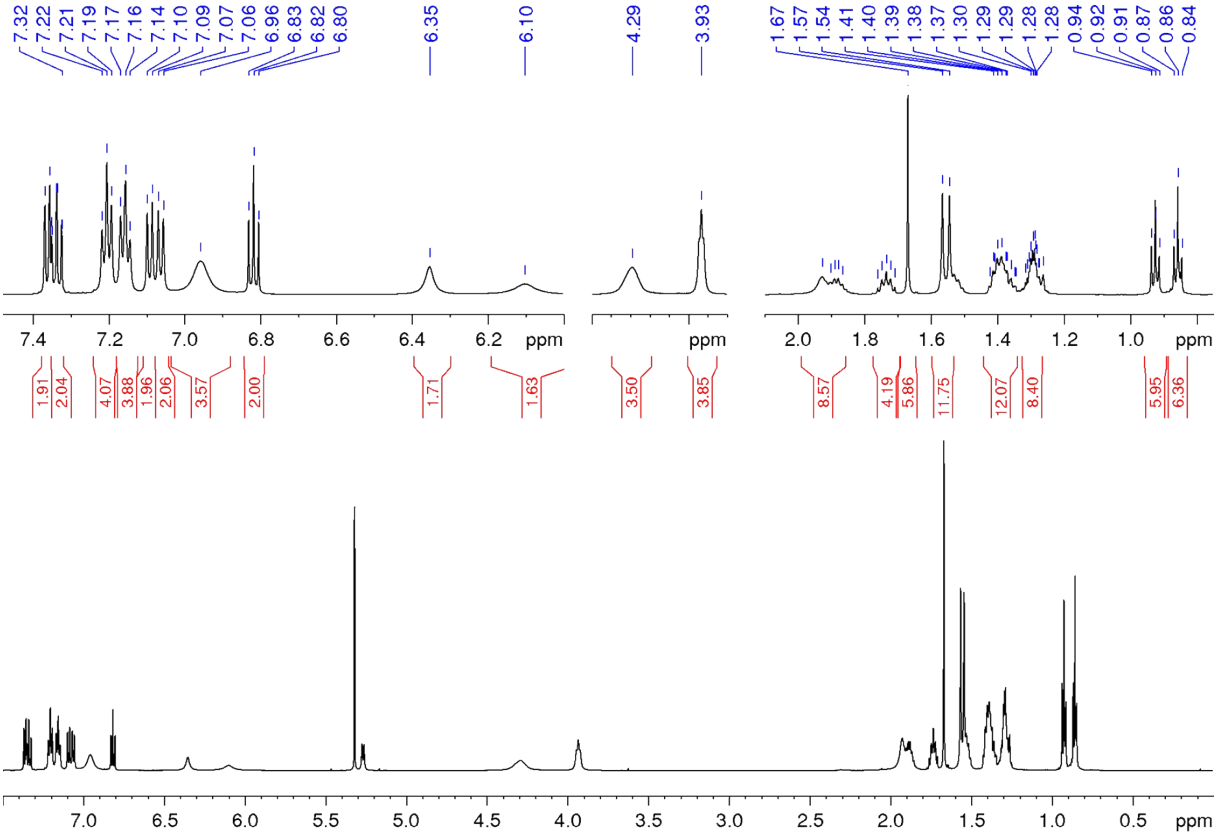

Fig. S43 ^{1}H NMR spectrum of **dSQB**.

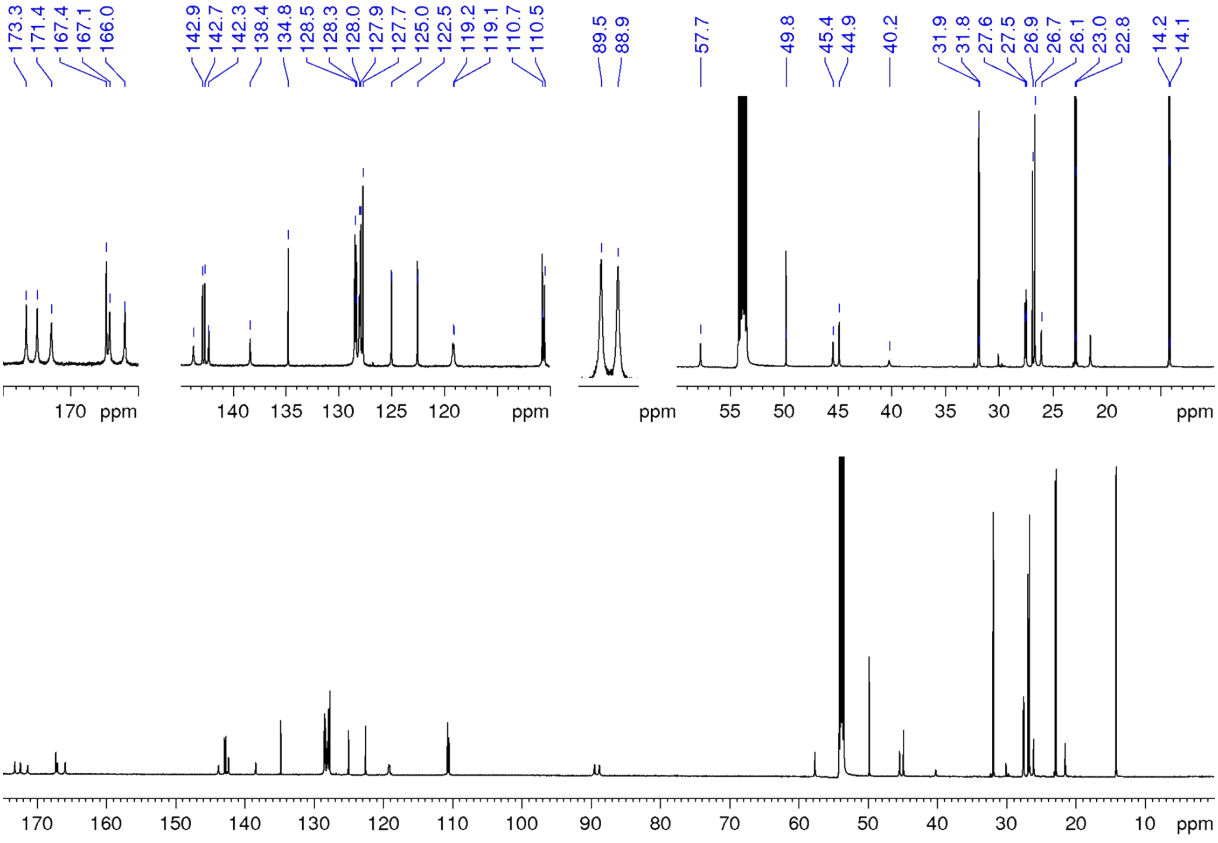

Fig. S44 ^{13}C NMR spectrum of **dSQB**.

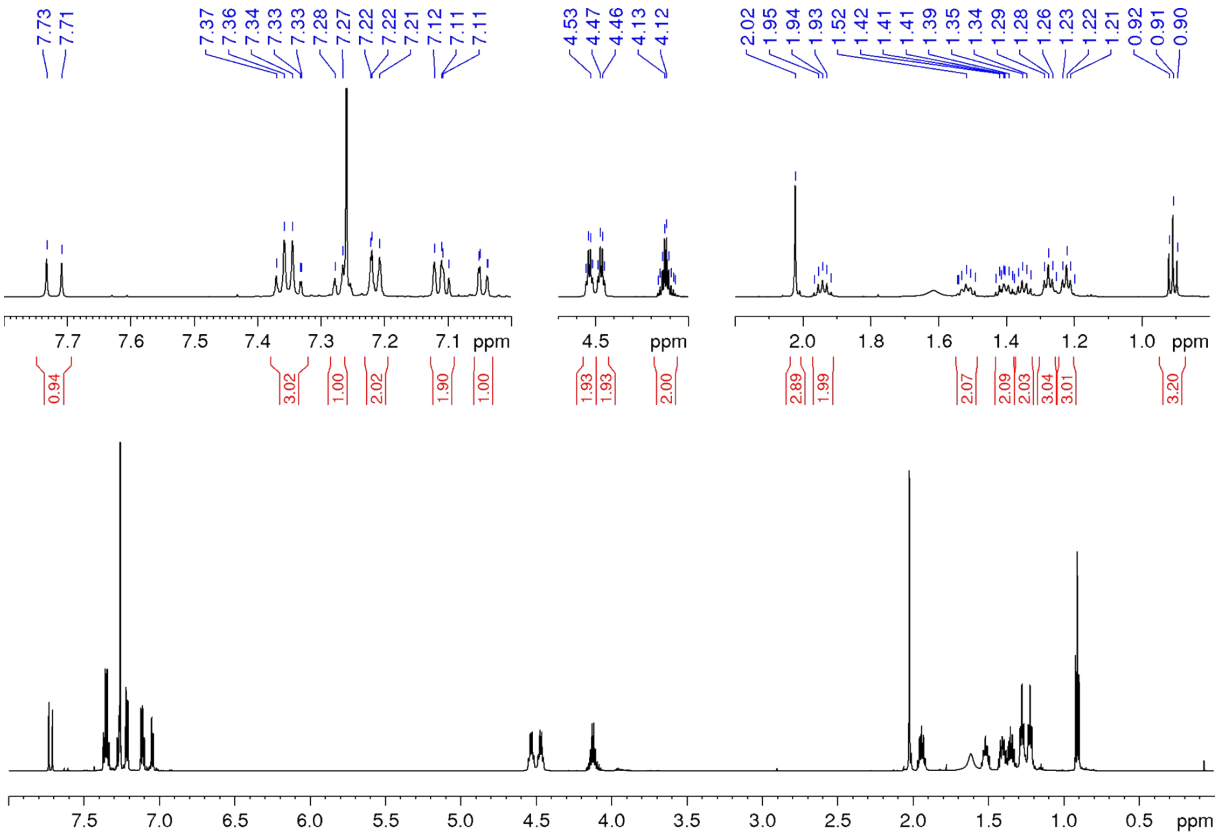

Fig. S45 ^{1}H NMR spectrum of **mMC**.

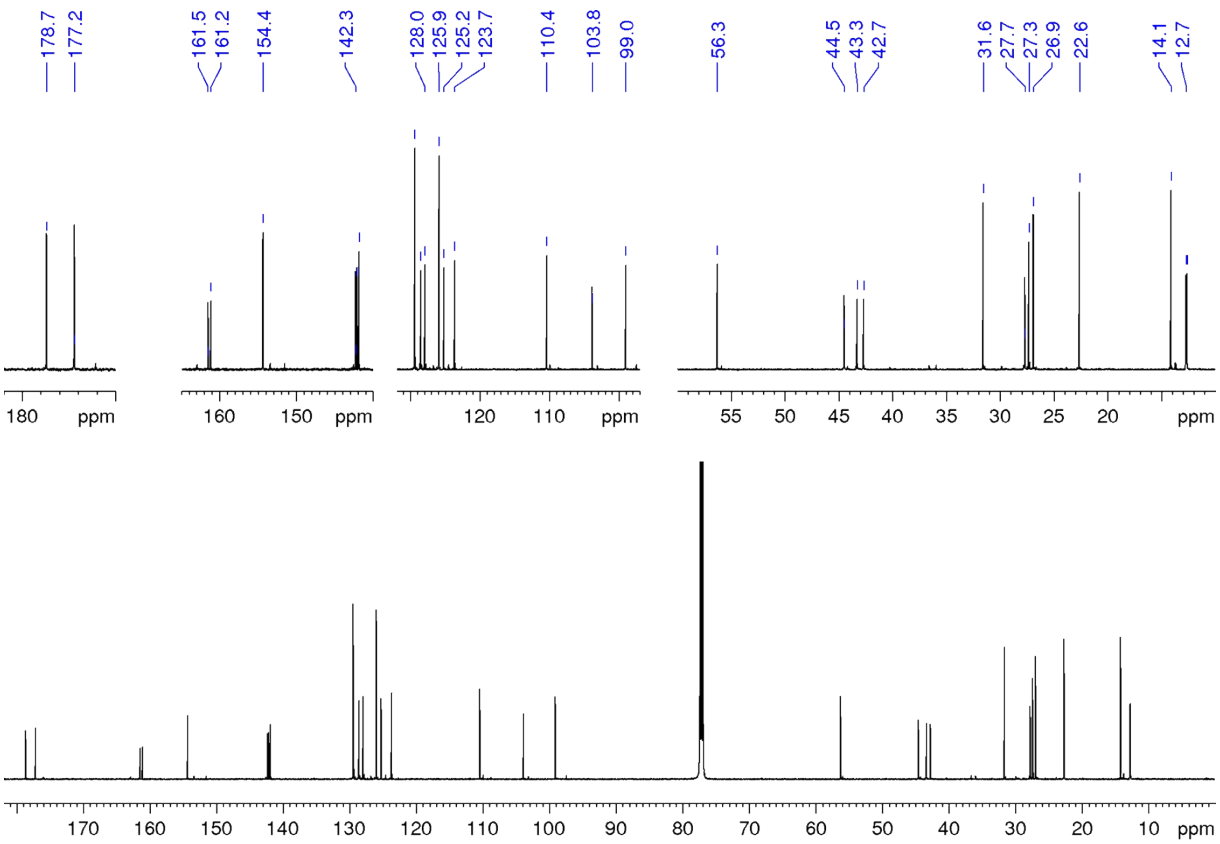

Fig. S46 ^{13}C NMR spectrum of **mMC**.

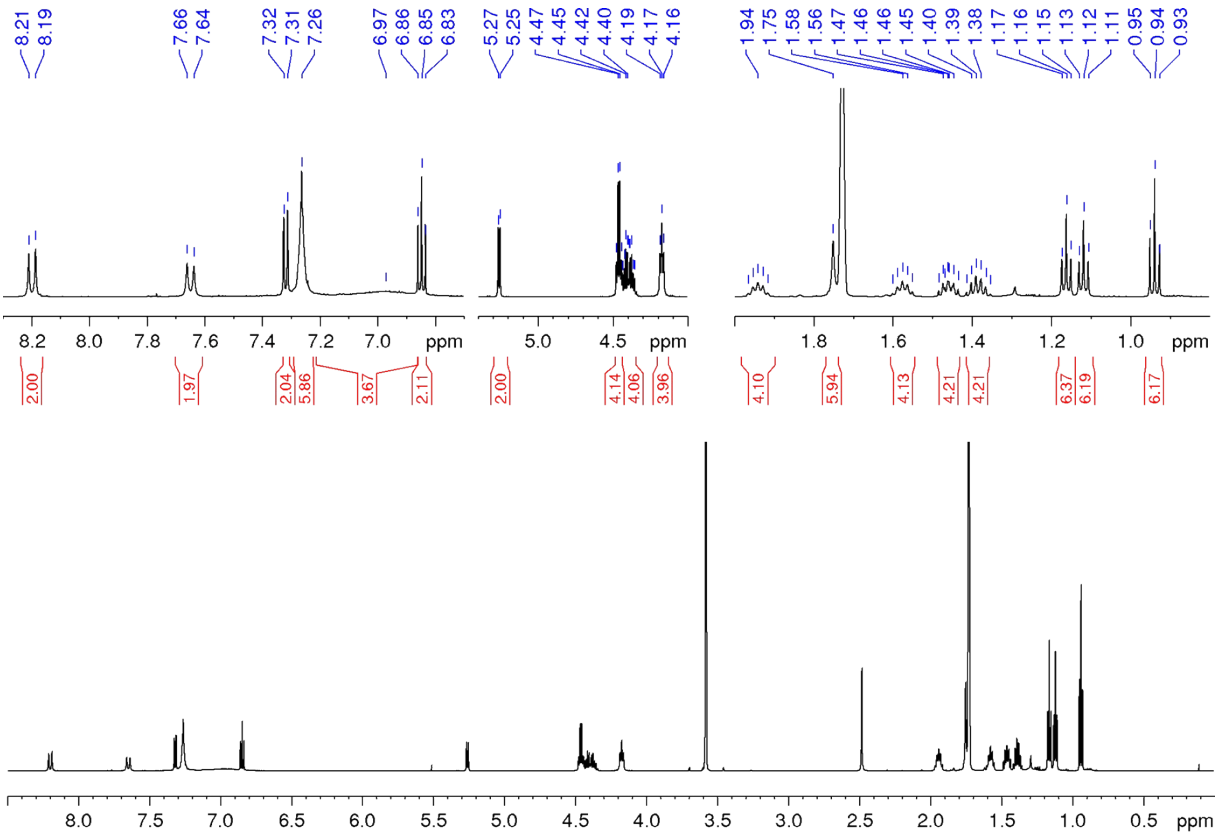

Fig. S47 ^{1}H NMR spectrum of **dMC**.

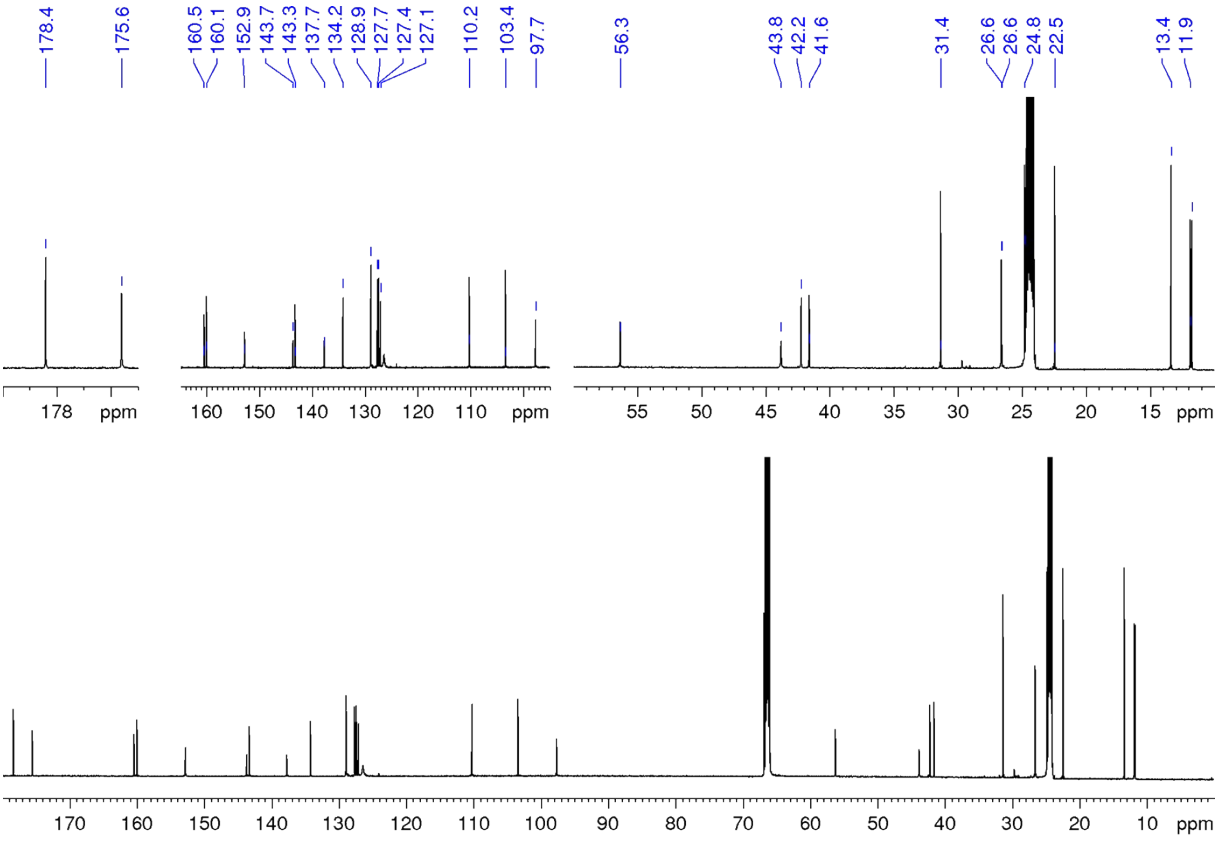

Fig. S48 ^{13}C NMR spectrum of **dMC**.

References

1. T.-S. Ahn, R. O. Al-Kaysi, A. M. Müller, K. M. Wentz and C. J. Bardeen, *Rev. Sci. Instrum.*, 2007, **78**, 086105.
2. M. J. Frisch, G. W. Trucks, H. B. Schlegel, G. E. Scuseria, M. A. Robb, J. R. Cheeseman, G. Scalmani, V. Barone, B. Mennucci, G. A. Petersson, H. Nakatsuji, M. Caricato, X. Li, H. P. Hratchian, A. F. Izmaylov, J. Bloino, G. Zheng, J. L. Sonnenberg, M. Hada, M. Ehara, K. Toyota, R. Fukuda, J. Hasegawa, M. Ishida, T. Nakajima, Y. Honda, O. Kitao, H. Nakai, T. Vreven, J. A. Montgomery Jr., J. E. Peralta, F. Ogliaro, M. J. Bearpark, J. J. Heyd, E. N. Brothers, K. N. Kudin, V. N. Staroverov, T. A. Keith, R. Kobayashi, J. Normand, K. Raghavachari, A. P. Rendell, J. C. Burant, S. S. Iyengar, J. Tomasi, M. Cossi, N. Rega, J. M. Millam, M. Klene, J. E. Knox, J. B. Cross, V. Bakken, C. Adamo, J. Jaramillo, R. Gomperts, R. E. Stratman, O. Yazyev, A. J. Austin, R. Cammi, C. Pomelli, J. W. Ochterski, R. L. Martin, K. Morokuma, V. G. Zakrzewski, G. A. Voth, P. Salvador, J. J. Dannenberg, S. Dapprich, A. D. Daniels, O. Farkas, J. B. Foresman, J. V. Ortiz, J. Cioslowski and D. J. Fox, Gaussian, Inc., Revision D.01 edn., 2010.
3. E. Richmond, K. B. Ling, N. Duguet, L. B. Manton, N. Çelebi-Ölçüm, Y.-H. Lam, S. Alsancak, A. M. Z. Slawin, K. N. Houk and A. D. Smith, *Org. Biomol. Chem.*, 2015, **13**, 1807-1817.
4. E. Castiglioni, S. Abbate, F. Lebon and G. Longhi, *Chirality*, 2012, **24**, 725-730.
5. G. Longhi, E. Castiglioni, J. Koshoubu, G. Mazzeo and S. Abbate, *Chirality*, 2016, **28**, 696-707.
6. D. Scherer, R. Dörfler, A. Feldner, T. Vogtmann, M. Schwoerer, U. Lawrenzt, W. Grahn and C. Lambert, *Chem. Phys.*, 2002, **279**, 179-207.
7. L. Beverina, R. Ruffo, C. M. Mari, G. A. Pagani, M. Sassi, F. De Angelis, S. Fantacci, J.-H. Yum, M. Grätzel and M. K. Nazeeruddin, *ChemSusChem*, 2009, **2**, 621-624.
8. T. Maeda, S. Nitta, Y. Sano, S. Tanaka, S. Yagi and H. Nakazumi, *Dyes Pigm.*, 2015, **122**, 160-167.
9. S. F. Völker, S. Uemura, M. Limpinsel, M. Mingebach, C. Deibel, V. Dyakonov and C. Lambert, *Macromol. Chem. Phys.*, 2010, **211**, 1098-1108.
10. M. H. Schreck, L. Breitschwerdt, H. Marciniak, M. Holzapfel, D. Schmidt, F. Würthner and C. Lambert, *Phys. Chem. Chem. Phys.*, 2019, **21**, 15346-15355.
11. D. V. Pestov, V. I. Slesarev, A. I. Ginak and V. I. Slesareva, *Chem. heterocycl. compounds*, 1988, **24**, 782-786.
12. A. J. Kay, A. D. Woolhouse, G. J. Gainsford, T. G. Haskell, T. H. Barnes, I. T. McKinnie and C. P. Wyss, *J. Mater. Chem.*, 2001, **11**, 996-1002.